



# Convergence analysis of a second-order semi-implicit projection method for Landau-Lifshitz equation

Jingrun Chen<sup>a</sup>, Cheng Wang<sup>b</sup>, Changjian Xie<sup>a</sup>

<sup>a</sup> School of Mathematical Sciences, Soochow University, Suzhou, China

<sup>b</sup> Mathematics Department, University of Massachusetts, North Dartmouth, MA 02747, USA



## ARTICLE INFO

### Article history:

Received 14 May 2019

Received in revised form 20 April 2021

Accepted 28 May 2021

Available online 3 June 2021

### Keywords:

Landau-Lifshitz equation

Backward differentiation formula

Semi-implicit scheme

Second-order accuracy

## ABSTRACT

The numerical approximation for the Landau-Lifshitz equation, which models the dynamics of the magnetization in a ferromagnetic material, is taken into consideration. This highly nonlinear equation, with a non-convex constraint, has several equivalent forms, and involves solving an auxiliary problem in the infinite domain. All these features have posed interesting challenges in developing numerical methods. In this paper, we first present a fully discrete semi-implicit method for solving the Landau-Lifshitz equation based on the second-order backward differentiation formula and the one-sided extrapolation (using previous time-step numerical values). A projection step is further used to preserve the length of the magnetization. Subsequently, we provide a rigorous convergence analysis for the fully discrete numerical solution by the introduction of two sets of approximated solutions where one set of solutions solves the Landau-Lifshitz equation and the other is projected onto the unit sphere. Second-order accuracy in both time and space is obtained provided that the spatial step-size is the same order as the temporal step-size. And also, the unique solvability of the numerical solution without any assumption for the step-size in both time and space is theoretically justified, using a monotonicity analysis. All these theoretical properties are verified by numerical examples in both 1D and 3D spaces.

© 2021 IMACS. Published by Elsevier B.V. All rights reserved.

## 1. Introduction

Micromagnetics is a continuum theory describing magnetization patterns inside ferromagnetic media. The dynamics of magnetization is governed by the Landau-Lifshitz (LL) equation [35]. This highly nonlinear equation indicates a non-convex constraint, which has always been a well-known difficulty in the numerical analysis. And also, this equation has several equivalent forms, and an auxiliary problem in the infinite domain has to be involved. All these features have posed interesting challenges in developing numerical methods. In the past several decades, many works have focused on the mathematical theory and numerical analysis of the LL equation [34,37,43]. The solvability of LL-type equations can be found in [26,40,44]; two structures of the solution regularity have been investigated. In the framework of weak solution, the existence of global weak solution in  $\mathbb{R}^3$  was proved in [6] and in [27] on a bounded domain  $\Omega \subset \mathbb{R}^2$ ; the nonuniqueness of weak solutions was demonstrated in [6] as well. In the framework of strong solution, local existence and uniqueness, and global existence and uniqueness with small-energy initial data for strong solutions to the LL equation in  $\mathbb{R}^3$  was shown in [12]. Local existence and uniqueness of strong solutions on a bounded domain  $\Omega$  was proved in [11]; global existence

E-mail addresses: [jingrunchen@suda.edu.cn](mailto:jingrunchen@suda.edu.cn) (J. Chen), [cwang1@umassd.edu](mailto:cwang1@umassd.edu) (C. Wang), [20184007005@stu.suda.edu.cn](mailto:20184007005@stu.suda.edu.cn) (C. Xie).

and uniqueness of strong solutions for small-energy initial data on a 2-D bounded domain was established, provided that  $\|\nabla \mathbf{m}_0\|_{H^1(\Omega)}$  is small enough for the bounded domain  $\Omega \subset \mathbb{R}^2$ . A similar uniqueness analysis was provided in [38] as well. We may refer to [27,52] for the existence of unique local strong solution.

Accordingly, numerous numerical approaches have been proposed to demonstrate the mathematical theory; review articles could be found in [16,34]. The first finite element work was introduced by Alouges and his collaborators [2,3,5], in which rigorous convergence proof was included with first-order accuracy in time and second-order accuracy in space. This method was further developed to reach almost the second-order temporal accuracy [4,33]. In another finite element work by Bartels and Prohl [7], they presented an implicit time integration method with second-order accuracy and unconditional stability. However, a nonlinear solver is needed at each time step, and a step-size condition  $k = \mathcal{O}(h^2)$  is needed to guarantee the existence of the solution for the fixed point iteration (with  $k$  the temporal step-size and  $h$  the spatial mesh-size), which is highly restrictive. In fact, a theoretical justification of the unique solvability of the numerical solution is expected to come from the convergence of the fixed-point iteration by applying Banach fixed-point theorem, under the CFL-like condition  $k = \mathcal{O}(h^2)$ . A similar finite element scheme was reported by Cimrák [17]. Again, a nonlinear solver is necessary at each time step, and the same step-size condition has to be imposed. Also see the related finite element works [1,21], as well as the corresponding analysis. Meanwhile, the existing works of finite difference method to the LL equation may be referred to [20,23,28,31,51]. In [20], a time stepping method in the form of a projection method was proposed; this method is implicit and unconditionally stable, and the rigorous proof was provided with the first-order accuracy in time and second-order accuracy in space. In [28], an updated source term was used, and an iteration algorithm was repeatedly performed until the numerical solution converges. In [31], the explicit and implicit mimetic finite difference algorithm was developed.

Regarding to the temporal discretization, the first kind of time-stepping scheme is the Gauss-Seidel projection method proposed by Wang, García-Cervera, and E [48], in which  $|\nabla \mathbf{m}|^2$  was treated as the Lagrange multiplier for the non-convex constraint  $|\mathbf{m}| = 1$  in the pointwise sense with  $\mathbf{m}$  the magnetization vector field. The resulting method is first-order accurate in time and is unconditionally stable. The second kind of time-stepping scheme is called geometric integration method. In [30], Jiang, Kaper, and Leaf developed the semi-analytic integration method by analytically integrating the system of ODEs, obtained after a spatial discretization of the LL equation. This is an explicit method with first-order accuracy, hence is subject to a CFL constraint,  $k = \mathcal{O}(h^2)$ . Such an approach has been applied in [32] (which yields the same numerical solution as the mid-point method, with second-order accuracy in time), and in a more general setting in [36] using the Cayley transform to lift the LL equation to the Lie algebra of the 3D rotation group. In addition, the first, second and fourth-order accurate temporal approximations were examined in [36], which is more amenable for building numerical schemes with the high-order accuracy. The third kind of time-stepping scheme is called the mid-point method [9,19], which is second-order accurate, unconditionally stable, and preserves the Lyapunov and Hamiltonian structures of the LL equation. Moreover, the fourth kind of time-stepping method is the high-order Runge-Kutta algorithms [41]. Also see other related works [18,22,29,33], etc. In fact, there have been many existing numerical works, in which a time step constraint  $k = \mathcal{O}(h^2)$  has to be imposed, such as explicit numerical schemes [3,30] (so that the constraint  $k = \mathcal{O}(h^2)$  has played a role of CFL condition), the fully implicit schemes [7,23,40] (so that a nonlinear solver is needed), and a fixed point iteration approach [18], etc.

Based on the linearity of the discrete system, we can also classify numerical methods into the explicit scheme [3,30], the fully implicit scheme [7,23,40] and the semi-implicit scheme [15,20,24,36,48]. In particular, the semi-discrete schemes are introduced in [40] for 2-D and in [15] for 3D formulation of the LL equation. Error estimates are derived under the existence assumption for the strong solution.

From the perspective of convergence analysis, it is worthy of mentioning [18], in which the fixed point iteration technique was used for handling the nonlinearities; the second-order convergence in time was proved, and was confirmed by numerical examples. It is noticed that, for all above-mentioned works with the established convergence analysis, a nonlinear solver has to be used at each time step, for the sake of numerical stability. However, the unique solvability analysis for these nonlinear numerical schemes has been a very challenging issue at the theoretical level, due to the highly complicated form in the nonlinear term. The only relevant analysis was reported in [23], in which the unique solvability was proved under a very restrictive condition,  $k \leq Ch^2$ . And also, a projection step has been used in many existing works, to preserve the length of the magnetization. Its nonlinear nature makes a theoretical analysis highly non-trivial. In turn, a derivation of the following numerical scheme is greatly desired: second-order accuracy in time and linearity of the scheme at each time step, so that the length of magnetization is preserved in the pointwise sense, and an optimal rate error estimate and unconditionally unique solvability analysis could be established at a theoretical level.

In this work, we propose and analyze a second-order accurate scheme that satisfies these desired properties. The second-order backward differentiation formula (BDF) approximation is applied to obtain an intermediate magnetization  $\tilde{\mathbf{m}}$ , and the right-hand-side nonlinear terms are treated in a semi-implicit style with a second-order extrapolation applied to the explicit coefficients. Such a numerical algorithm leads to a linear system of equations with variable coefficients to solve at each time step. Its unconditionally unique solvability (no condition is needed for the temporal stepsize in terms of spatial stepsize) is guaranteed by a careful application of the monotonicity analysis, the so-called Browder-Minty lemma. A projection step is further used to preserve the unit length of magnetization at each time step, which poses a non-convex constraint. More importantly, we provide a rigorous convergence and error estimate, by the usage of the linearized stability analysis for the numerical error functions. In particular, we notice that, an *a priori*  $W_h^{1,\infty}$  bound assumption for the numerical solution at the previous time steps has to be imposed to pass through the convergence analysis. As a consequence, the standard  $L^2$

error estimate is insufficient to recover such a bound for the numerical solution. Instead, we have to perform the  $H^1$  error estimate, and such a  $W_h^{1,\infty}$  bound could be obtained at the next time step as a consequence of the  $H^1$  estimate, via the help of the inverse inequality combined with a mild time stepsize condition  $k = \mathcal{O}(h)$ . Careful error estimates for both the original magnetization  $\mathbf{m}$  and the intermediate magnetization  $\tilde{\mathbf{m}}$  have to be taken into consideration at the projection step (a highly nonlinear operation). To the best of our knowledge, it is the first such result to report an optimal convergence analysis with second order accuracy in both time and space.

The rest of this paper is organized as follows. In Section 2, we introduce the fully discrete numerical scheme and state the main theoretical results: unique solvability analysis and optimal rate convergence analysis. Detailed proofs are also provided in this section. Numerical results are presented in Section 3, including both the 1D and 3D examples to confirm the theoretical analysis. Conclusions are drawn in Section 4.

## 2. Main theoretical results

The LL equation reads as

$$\mathbf{m}_t = -\mathbf{m} \times \Delta \mathbf{m} - \alpha \mathbf{m} \times (\mathbf{m} \times \Delta \mathbf{m}) \tag{2.1}$$

with

$$\frac{\partial \mathbf{m}}{\partial \mathbf{v}} \Big|_{\Gamma} = 0, \tag{2.2}$$

where  $\Gamma = \partial\Omega$  and  $\mathbf{v}$  is the unit outward normal vector along  $\Gamma$ . Here  $\mathbf{m} : \Omega \subset \mathbb{R}^d \rightarrow S^2$  represents the magnetization vector field with  $|\mathbf{m}| = 1, \forall x \in \Omega, d = 1, 2, 3$  is the spatial dimension, and  $\alpha > 0$  is the damping parameter. The first term on the right hand side of (2.1) is the gyromagnetic term, and the second term is the damping term. Compared to the original LL equation [35], (2.1) only includes the exchange term which poses the main difficulty in numerical analysis, as done in the literature [7,18,20,24]. Application of the scheme (2.5) to the original LL equation under external fields will be presented in another publication [50]. To ease the presentation, we set  $\Omega = [0, 1]^d$ , in which  $d$  is the dimension.

### 2.1. Finite difference discretization and the fully discrete scheme

The finite difference method is used to approximate (2.1) and (2.2). Denote the spatial step-size by  $h$  in the 1D case and divide  $[0, 1]$  into  $N_x$  equal segments; see the schematic mesh in Fig. 1. Define  $x_i = ih, i = 0, 1, 2, \dots, N_x$ , with  $x_0 = 0, x_{N_x} = 1$ , and  $\hat{x}_i = x_{i-\frac{1}{2}} = (i - \frac{1}{2})h, i = 1, \dots, N_x$ . Denote the magnetization obtained by the numerical scheme at  $(\hat{x}_i, t^n)$  by  $\mathbf{m}_i^n$ , in which we have introduced  $t^n = nk$ , with  $k$  being the temporal step-size, and  $n \leq \lfloor \frac{T}{k} \rfloor, T$  being the final time. To approximate the boundary condition (2.2), we introduce ghost points  $x_{-\frac{1}{2}}, x_{N_x+\frac{1}{2}}$  and apply Taylor expansions for  $x_{-\frac{1}{2}}, x_{\frac{1}{2}}$  at  $x_0$ , and  $x_{N_x+\frac{1}{2}}, x_{N_x-\frac{1}{2}}$  at  $x_{N_x}$ , respectively. We then obtain a third order extrapolation formula:

$$\mathbf{m}_1 = \mathbf{m}_0, \quad \mathbf{m}_{N_x+1} = \mathbf{m}_{N_x}.$$

In the 3D case, we have spatial stepsizes  $h_x = \frac{1}{N_x}, h_y = \frac{1}{N_y}, h_z = \frac{1}{N_z}$  and grid points  $(\hat{x}_i, \hat{y}_j, \hat{z}_k)$ , with  $\hat{x}_i = x_{i-\frac{1}{2}} = (i - \frac{1}{2})h_x, \hat{y}_j = y_{j-\frac{1}{2}} = (j - \frac{1}{2})h_y$  and  $\hat{z}_k = z_{k-\frac{1}{2}} = (k - \frac{1}{2})h_z (0 \leq i \leq N_x + 1, 0 \leq j \leq N_y + 1, 0 \leq k \leq N_z + 1)$ . The extrapolation formula along the  $z$  direction near  $z = 0$  and  $z = 1$  is

$$\mathbf{m}_{i,j,1} = \mathbf{m}_{i,j,0}, \quad \mathbf{m}_{i,j,N_z+1} = \mathbf{m}_{i,j,N_z}. \tag{2.3}$$

Extrapolation formulas for the boundary condition along other directions can be derived similarly.

In addition, given  $\mathbf{m}_e(\cdot, t = 0)$  as the exact initial data at  $t = 0$  (with  $\mathbf{m}_e$  the exact solution), the numerical initial data for  $\mathbf{m}$  is set as

$$\mathbf{m}_{i,j,k}^0 = \mathcal{P}_h \mathbf{m}_e(\hat{x}_i, \hat{y}_j, \hat{z}_k, t = 0), \quad \mathcal{P}_h \text{ is the point-wise interpolation.} \tag{2.4}$$

The standard second-order centered difference applied to  $\Delta \mathbf{m}$  results in

$$\begin{aligned} \Delta_h \mathbf{m}_{i,j,k} &= \frac{\mathbf{m}_{i+1,j,k} - 2\mathbf{m}_{i,j,k} + \mathbf{m}_{i-1,j,k}}{h_x^2} \\ &+ \frac{\mathbf{m}_{i,j+1,k} - 2\mathbf{m}_{i,j,k} + \mathbf{m}_{i,j-1,k}}{h_y^2} \\ &+ \frac{\mathbf{m}_{i,j,k+1} - 2\mathbf{m}_{i,j,k} + \mathbf{m}_{i,j,k-1}}{h_z^2}, \end{aligned}$$

and the discrete gradient operator  $\nabla_h \mathbf{m}$  with  $\mathbf{m} = (u, v, w)^T$  reads as

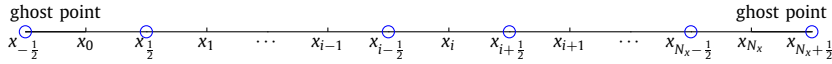


Fig. 1. Illustration of the 1D spatial mesh.

$$\nabla_h \mathbf{m}_{i,j,k} = \begin{bmatrix} \frac{u_{i+1,j,k} - u_{i,j,k}}{h_x} & \frac{v_{i+1,j,k} - v_{i,j,k}}{h_x} & \frac{w_{i+1,j,k} - w_{i,j,k}}{h_x} \\ \frac{u_{i,j+1,k} - u_{i,j,k}}{h_y} & \frac{v_{i,j+1,k} - v_{i,j,k}}{h_y} & \frac{w_{i,j+1,k} - w_{i,j,k}}{h_y} \\ \frac{u_{i,j,k+1} - u_{i,j,k}}{h_z} & \frac{v_{i,j,k+1} - v_{i,j,k}}{h_z} & \frac{w_{i,j,k+1} - w_{i,j,k}}{h_z} \end{bmatrix}.$$

Denote the temporal stepsize by  $k$ , and define  $t^n = nk, n \leq \lfloor \frac{T}{k} \rfloor$  with  $T$  the final time. The second-order BDF approximation is applied to the temporal derivative:

$$\frac{\frac{3}{2} \mathbf{m}_h^{n+2} - 2 \mathbf{m}_h^{n+1} + \frac{1}{2} \mathbf{m}_h^n}{k} = \frac{\partial}{\partial t} \mathbf{m}_h^{n+2} + \mathcal{O}(k^2).$$

Note that the right hand side of the above equation is evaluated at  $t^{n+2}$ , a direct application of the BDF method leads to a fully nonlinear scheme. To overcome this difficulty, we come up with a semi-implicit scheme, in which the nonlinear coefficient is approximated by the second-order extrapolation formula:

$$\begin{aligned} \frac{\frac{3}{2} \mathbf{m}_h^{n+2} - 2 \mathbf{m}_h^{n+1} + \frac{1}{2} \mathbf{m}_h^n}{k} &= - \left( 2 \mathbf{m}_h^{n+1} - \mathbf{m}_h^n \right) \times \Delta_h \mathbf{m}_h^{n+2} \\ &\quad - \alpha \left( 2 \mathbf{m}_h^{n+1} - \mathbf{m}_h^n \right) \times \left( 2 \mathbf{m}_h^{n+1} - \mathbf{m}_h^n \right) \times \Delta_h \mathbf{m}_h^{n+2}. \end{aligned} \tag{2.5}$$

A projection step is then added to preserve the length of magnetization. This scheme has been used to study domain wall dynamics under external magnetic fields [50]. However, this scheme is difficult to conduct the convergence analysis due to the lack of numerical stability of Lax-Richtmyer type. To overcome this difficulty, we separate the time-marching step and the projection step in the following way, namely Algorithm 2.1:

$$\hat{\mathbf{m}}_h^{n+2} = 2 \mathbf{m}_h^{n+1} - \mathbf{m}_h^n, \tag{2.6}$$

$$\begin{aligned} \frac{\frac{3}{2} \tilde{\mathbf{m}}_h^{n+2} - 2 \tilde{\mathbf{m}}_h^{n+1} + \frac{1}{2} \tilde{\mathbf{m}}_h^n}{k} &= - \hat{\mathbf{m}}_h^{n+2} \times \Delta_h \tilde{\mathbf{m}}_h^{n+2} \\ &\quad - \alpha \hat{\mathbf{m}}_h^{n+2} \times (\hat{\mathbf{m}}_h^{n+2} \times \Delta_h \tilde{\mathbf{m}}_h^{n+2}), \end{aligned} \tag{2.7}$$

$$\mathbf{m}_h^{n+2} = \frac{\tilde{\mathbf{m}}_h^{n+2}}{|\tilde{\mathbf{m}}_h^{n+2}|}. \tag{2.8}$$

The discrete boundary condition (2.3) is imposed for  $\tilde{\mathbf{m}}_h^{n+2}$  in (2.7). In fact, this boundary condition could be rewritten as  $(\nabla_h \tilde{\mathbf{m}}_h^{n+2} \cdot \mathbf{n})|_{\partial\Omega} = 0$ .

**Remark 2.1.** To kick start the iteration of our method, we can use the first-order semi-implicit projection scheme using the first-order BDF and the first-order one-sided interpolation and the method is still second-order accurate.

**Remark 2.2.** We use the sparse LU factorization solver and also the Generalized Minimum Residual Method to solve the linear system in (2.7).

2.2. Some notations and the main theoretical results

For simplicity of presentation, we assume that  $N_x = N_y = N_z = N$  so that  $h_x = h_y = h_z = h$ . An extension to the general case is straightforward. In the finite difference approximation, all the numerical values are assigned on the numerical grid points. As a result, the discrete grid functions (with notations  $\mathbf{f}_h, \mathbf{g}_h$ ), which are only defined over the corresponding numerical grid points, are introduced.

First, we introduce the discrete  $\ell^2$  inner product and discrete  $\|\cdot\|_2$  norm.

**Definition 2.1** (Inner product and  $\|\cdot\|_2$  norm). For grid functions  $\mathbf{f}_h$  and  $\mathbf{g}_h$  over the uniform numerical grid, we define

$$\langle \mathbf{f}_h, \mathbf{g}_h \rangle = h^d \sum_{\mathcal{I} \in \Lambda_d} \mathbf{f}_{\mathcal{I}} \cdot \mathbf{g}_{\mathcal{I}}, \tag{2.9}$$

where  $\Lambda_d$  is the index set and  $\mathcal{I}$  is the index which closely depends on  $d$ . In turn, the discrete  $\|\cdot\|_2$  norm is given by

$$\|\mathbf{f}_h\|_2 = (\langle \mathbf{f}_h, \mathbf{f}_h \rangle)^{1/2}. \tag{2.10}$$

In addition, the discrete  $H_h^1$ -norm is given by  $\|\mathbf{f}_h\|_{H_h^1}^2 := \|\mathbf{f}_h\|_2^2 + \|\nabla_h \mathbf{f}_h\|_2^2$ .

**Definition 2.2** (Discrete  $\|\cdot\|_\infty$  norm). For the grid function  $\mathbf{f}_h$  over the uniform numerical grid, we define

$$\|\mathbf{f}_h\|_\infty = \max_{\mathcal{I} \in \Lambda_d} \|\mathbf{f}_{\mathcal{I}}\|_\infty.$$

**Definition 2.3.** For the grid function  $\mathbf{f}_h$ , we define the average of summation as

$$\overline{\mathbf{f}}_h = h^d \sum_{\mathcal{I} \in \Lambda_d} \mathbf{f}_{\mathcal{I}}.$$

**Definition 2.4.** For any grid function  $\mathbf{f}_h$  with  $\overline{\mathbf{f}}_h = 0$ , a discrete inverse Laplacian operator is defined as:  $\boldsymbol{\psi}_h = (-\Delta_h)^{-1} \mathbf{f}_h$  is the unique grid function satisfying

$$-\Delta_h \boldsymbol{\psi}_h = \mathbf{f}_h, \quad (\nabla_h \boldsymbol{\psi}_h \cdot \mathbf{n})|_{\partial\Omega} = 0, \quad \overline{\boldsymbol{\psi}}_h = 0.$$

It is noticed that the zero-average constraint,  $\overline{\boldsymbol{\psi}}_h = 0$ , makes the operator  $(-\Delta_h)^{-1}$  uniquely defined. In turn, a discrete  $H_h^{-1}$ -norm is introduced for any  $\mathbf{f}_h$  with  $\overline{\mathbf{f}}_h = 0$ :

$$\|\mathbf{f}_h\|_{-1}^2 = \langle (-\Delta_h)^{-1} \mathbf{f}_h, \mathbf{f}_h \rangle.$$

The first theoretical result is the unique solvability analysis of scheme (2.6)-(2.8). We observe that the unique solvability for (2.7) could be simplified as the analysis for

$$\frac{\frac{3}{2} \tilde{\mathbf{m}}_h - \mathbf{p}_h}{k} = -\hat{\mathbf{m}}_h \times \Delta_h \tilde{\mathbf{m}}_h - \alpha \hat{\mathbf{m}}_h \times (\hat{\mathbf{m}}_h \times \Delta_h \tilde{\mathbf{m}}_h), \tag{2.11}$$

with  $\mathbf{p}_h, \hat{\mathbf{m}}_h$  given.

**Theorem 2.1.** Given  $\mathbf{p}_h, \hat{\mathbf{m}}_h$ , the numerical scheme (2.11) is uniquely solvable.

The second theoretical result is the optimal rate convergence analysis.

**Theorem 2.2.** Let  $\mathbf{m}_e \in C^3([0, T]; C^1) \cap C^1([0, T]; C^3) \cap L^\infty([0, T]; C^5)$  be the exact solution of (2.1) with the initial data  $\mathbf{m}_e(\mathbf{x}, 0) = \mathbf{m}_e^0(\mathbf{x})$  and  $\mathbf{m}_h$  be the numerical solution of the equation (2.6)-(2.8) with the initial data  $\mathbf{m}_h^0 = \mathbf{m}_{e,h}^0$  and  $\mathbf{m}_h^1 = \mathbf{m}_{e,h}^1$ . Suppose that the initial error satisfies  $\|\mathbf{m}_{e,h}^\ell - \mathbf{m}_h^\ell\|_2 + \|\nabla_h(\mathbf{m}_{e,h}^\ell - \mathbf{m}_h^\ell)\|_2 = \mathcal{O}(k^2 + h^2)$ ,  $\ell = 0, 1$ , and  $k \leq Ch$ . Then the following convergence result holds as  $h$  and  $k$  goes to zero:

$$\|\mathbf{m}_{e,h}^n - \mathbf{m}_h^n\|_2 + \|\nabla_h(\mathbf{m}_{e,h}^n - \mathbf{m}_h^n)\|_2 \leq C(k^2 + h^2), \quad \forall n \geq 2, \tag{2.12}$$

in which the constant  $C > 0$  is independent of  $k$  and  $h$ .

### 2.3. A few preliminary estimates

The proof of the standard inverse inequality and discrete Gronwall inequality could be obtained in existing textbooks; we just cite the results here. The inverse inequality presented in [14] is in the finite element version; its extension to the finite difference version is straightforward.

**Lemma 2.1.** (Inverse inequality) [14]. The inverse inequality implies that

$$\|\mathbf{e}_h^n\|_\infty \leq \gamma h^{-d/2} \|\mathbf{e}_h^n\|_2, \quad \|\nabla_h \mathbf{e}_h^n\|_\infty \leq \gamma h^{-d/2} \|\nabla_h \mathbf{e}_h^n\|_2,$$

in which constant  $\gamma$  depends on the form of the discrete  $\|\cdot\|_2$  norm. Under the definition (2.9) and (2.10) for the cell-centered grid function, such a constant could be taken as  $\gamma = 1$ .

**Lemma 2.2.** (Discrete Gronwall inequality) [25]. Let  $\{\alpha_j\}_{j \geq 0}, \{\beta_j\}_{j \geq 0}$  and  $\{\omega_j\}_{j \geq 0}$  be sequences of real numbers such that

$$\alpha_j \leq \alpha_{j+1}, \quad \beta_j \geq 0, \quad \text{and} \quad \omega_j \leq \alpha_j + \sum_{i=0}^{j-1} \beta_i \omega_i, \quad \forall j \geq 0.$$

Then it holds that

$$\omega_j \leq \alpha_j \exp \left\{ \sum_{i=0}^{j-1} \beta_i \right\}, \quad \forall j \geq 0.$$

**Lemma 2.3** (Summation by parts). For any grid functions  $\mathbf{f}_h$  and  $\mathbf{g}_h$ , with  $\mathbf{f}_h$  satisfying the discrete boundary condition (2.3), the following identity is valid:

$$\langle -\Delta_h \mathbf{f}_h, \mathbf{g}_h \rangle = \langle \nabla_h \mathbf{f}_h, \nabla_h \mathbf{g}_h \rangle. \tag{2.13}$$

**Proof.** For simplicity of presentation, we only focus on the 1D case; an extension to the 2D and 3D formulas will be straightforward. A careful calculation reveals that

$$\sum_{i=1}^N (\mathbf{g}_h)_i \cdot \frac{(\mathbf{f}_h)_{i-1} - 2(\mathbf{f}_h)_i + (\mathbf{f}_h)_{i+1}}{h^2} = - \sum_{i=1}^N \frac{(\mathbf{g}_h)_i - (\mathbf{g}_h)_{i-1}}{h} \cdot \frac{(\mathbf{f}_h)_i - (\mathbf{f}_h)_{i-1}}{h},$$

if  $\mathbf{f}_h$  satisfies the discrete boundary condition (2.3), i.e.,  $(\mathbf{f}_h)_0 = (\mathbf{f}_h)_1$ ,  $(\mathbf{f}_h)_{N+1} = (\mathbf{f}_h)_N$ . This identity is exactly the summation by parts formula (2.13). The proof of Lemma 2.3 is complete.  $\square$

The following estimate will be utilized in the convergence analysis. In the sequel, for simplicity of our notation, we will use the uniform constant  $\mathcal{C}$  to denote all the controllable constants in this paper.

**Lemma 2.4** (Discrete gradient acting on cross product). For grid functions  $\mathbf{f}_h$  and  $\mathbf{g}_h$  over the uniform numerical grid, we have

$$\|\nabla_h(\mathbf{f}_h \times \mathbf{g}_h)\|_2^2 \leq \mathcal{C} \left( \|\mathbf{f}_h\|_\infty^2 \cdot \|\nabla_h \mathbf{g}_h\|_2^2 + \|\mathbf{g}_h\|_\infty^2 \cdot \|\nabla_h \mathbf{f}_h\|_2^2 \right), \tag{2.14}$$

$$\langle (\mathbf{f}_h \times \Delta_h \mathbf{g}_h) \times \mathbf{f}_h, \mathbf{g}_h \rangle = \langle \mathbf{f}_h \times (\mathbf{g}_h \times \mathbf{f}_h), \Delta_h \mathbf{g}_h \rangle, \tag{2.15}$$

$$\langle \mathbf{f}_h \times (\mathbf{f}_h \times \mathbf{g}_h), \mathbf{g}_h \rangle = -\|\mathbf{f}_h \times \mathbf{g}_h\|_2^2. \tag{2.16}$$

**Proof.** Without loss of generality, we only look at the 1D case; an extension to the 3D case is straightforward. We begin with the following expansion

$$\begin{aligned} [\nabla_h(\mathbf{f}_h \times \mathbf{g}_h)]_{i+\frac{1}{2}} &= \frac{(\mathbf{f}_h)_{i+1} \times (\mathbf{g}_h)_{i+1} - (\mathbf{f}_h)_i \times (\mathbf{g}_h)_i}{h} \\ &= \frac{(\mathbf{f}_h)_{i+1} - (\mathbf{f}_h)_i}{h} \times (\mathbf{g}_h)_{i+1} + (\mathbf{f}_h)_i \times \frac{(\mathbf{g}_h)_{i+1} - (\mathbf{g}_h)_i}{h} \\ &= (\nabla_h \mathbf{f}_h)_{i+\frac{1}{2}} \times (\mathbf{g}_h)_{i+1} + (\mathbf{f}_h)_i \times (\nabla_h \mathbf{g}_h)_{i+\frac{1}{2}}. \end{aligned} \tag{2.17}$$

In turn, an application of the discrete Hölder inequality to (2.17) yields (2.14). Also note that

$$\begin{aligned} \langle (\mathbf{f}_h \times \Delta_h \mathbf{g}_h) \times \mathbf{f}_h, \mathbf{g}_h \rangle &= -\langle \mathbf{g}_h \times \mathbf{f}_h, \mathbf{f}_h \times \Delta_h \mathbf{g}_h \rangle \\ &= \langle \mathbf{f}_h \times (\mathbf{g}_h \times \mathbf{f}_h), \Delta_h \mathbf{g}_h \rangle, \end{aligned}$$

and

$$\begin{aligned} \langle \mathbf{f}_h \times (\mathbf{f}_h \times \mathbf{g}_h), \mathbf{g}_h \rangle &= \langle \mathbf{f}_h \times \mathbf{g}_h, \mathbf{g}_h \times \mathbf{f}_h \rangle \\ &= -\|\mathbf{f}_h \times \mathbf{g}_h\|_2^2. \quad \square \end{aligned}$$

The following estimate will be used in the error estimate at the projection step.

**Lemma 2.5.** Consider  $\mathbf{m}_h = \mathcal{P}_h \mathbf{m}_e + h^2 \mathbf{m}^{(1)}$ , in which  $\mathcal{P}_h$  stands for the point-wise interpolation of a continuous function over the numerical grid points, the continuous function  $\mathbf{m}_e$  satisfies a regularity requirement  $\|\mathbf{m}_e\|_{W^{1,\infty}} \leq \mathcal{C}$ ,  $|\mathbf{m}_e| = 1$  at a point-wise level, and the grid function  $\mathbf{m}^{(1)}$  satisfies  $\|\mathbf{m}^{(1)}\|_\infty + \|\nabla_h \mathbf{m}^{(1)}\|_\infty \leq \mathcal{C}$ . For any numerical solution  $\tilde{\mathbf{m}}_h$ , we define  $\mathbf{m}_h = \frac{\tilde{\mathbf{m}}_h}{|\tilde{\mathbf{m}}_h|}$ . Suppose both numerical profiles satisfy the following  $W_h^{1,\infty}$  bounds

$$|\tilde{\mathbf{m}}_h| \geq \frac{1}{2}, \quad \text{at a pointwise level}, \tag{2.18}$$

$$\|\mathbf{m}_h\|_\infty + \|\nabla_h \mathbf{m}_h\|_\infty \leq M, \quad \|\tilde{\mathbf{m}}_h\|_\infty + \|\nabla_h \tilde{\mathbf{m}}_h\|_\infty \leq M, \tag{2.19}$$

and we denote the numerical error functions as  $\mathbf{e}_h = \mathbf{m}_h - \underline{\mathbf{m}}_h$ ,  $\tilde{\mathbf{e}}_h = \tilde{\mathbf{m}}_h - \underline{\mathbf{m}}_h$ . Then the following estimate is valid

$$\|\mathbf{e}_h\|_2 \leq 2\|\tilde{\mathbf{e}}_h\|_2 + \mathcal{O}(h^2), \quad \|\nabla_h \mathbf{e}_h\|_2 \leq \mathcal{C}(\|\nabla_h \tilde{\mathbf{e}}_h\|_2 + \|\tilde{\mathbf{e}}_h\|_2) + \mathcal{O}(h^2). \tag{2.20}$$

**Proof.** A direct calculation shows that

$$\begin{aligned} \mathbf{e}_h &= \mathbf{m}_h - \underline{\mathbf{m}}_h = \frac{\tilde{\mathbf{m}}_h}{|\tilde{\mathbf{m}}_h|} - \underline{\mathbf{m}}_h = \tilde{\mathbf{m}}_h - \underline{\mathbf{m}}_h + \frac{\tilde{\mathbf{m}}_h}{|\tilde{\mathbf{m}}_h|} - \tilde{\mathbf{m}}_h \\ &= \tilde{\mathbf{e}}_h + \frac{\tilde{\mathbf{m}}_h}{|\tilde{\mathbf{m}}_h|} (|\underline{\mathbf{m}}_h| - |\tilde{\mathbf{m}}_h|) + \frac{\tilde{\mathbf{m}}_h}{|\tilde{\mathbf{m}}_h|} (1 - |\underline{\mathbf{m}}_h|). \end{aligned} \tag{2.21}$$

Since  $||\underline{\mathbf{m}}_h| - |\tilde{\mathbf{m}}_h|| \leq |\underline{\mathbf{m}}_h - \tilde{\mathbf{m}}_h|$ , we get

$$\left\| \tilde{\mathbf{e}}_h + \frac{\tilde{\mathbf{m}}_h}{|\tilde{\mathbf{m}}_h|} (|\underline{\mathbf{m}}_h| - |\tilde{\mathbf{m}}_h|) \right\|_2 \leq \|\tilde{\mathbf{e}}_h\|_2 + \|\tilde{\mathbf{e}}_h\|_2 = 2\|\tilde{\mathbf{e}}_h\|_2. \tag{2.22}$$

For the last term on the right hand side of (2.21), we observe that

$$|1 - |\underline{\mathbf{m}}_h|| = |\mathbf{m}_e| - |\underline{\mathbf{m}}_h| \leq |\mathbf{m}_e - \underline{\mathbf{m}}_h| = h^2 |\mathbf{m}^{(1)}| = \mathcal{O}(h^2), \tag{2.23}$$

which in turn yields

$$\left\| \frac{\tilde{\mathbf{m}}_h}{|\tilde{\mathbf{m}}_h|} (1 - |\underline{\mathbf{m}}_h|) \right\|_2 = \mathcal{O}(h^2). \tag{2.24}$$

As a result, a substitution of (2.22) and (2.24) into (2.21) leads to the first estimate in (2.20). For the second inequality, we notice that

$$\begin{aligned} \nabla_h \mathbf{e}_h &= \nabla_h \frac{\tilde{\mathbf{m}}_h}{|\tilde{\mathbf{m}}_h|} - \nabla_h \underline{\mathbf{m}}_h = \nabla_h \left[ \frac{\tilde{\mathbf{m}}_h}{|\tilde{\mathbf{m}}_h|} - \frac{\underline{\mathbf{m}}_h}{|\underline{\mathbf{m}}_h|} \right] + \nabla_h \left[ \frac{\underline{\mathbf{m}}_h}{|\underline{\mathbf{m}}_h|} - \underline{\mathbf{m}}_h \right] \\ &= \nabla_h \frac{\tilde{\mathbf{e}}_h}{|\tilde{\mathbf{m}}_h|} + \nabla_h \left[ \frac{\underline{\mathbf{m}}_h}{|\underline{\mathbf{m}}_h|} (1 - |\tilde{\mathbf{m}}_h|) \right]. \end{aligned} \tag{2.25}$$

The analysis for the first part is straightforward:

$$\left\| \nabla_h \frac{\tilde{\mathbf{e}}_h}{|\tilde{\mathbf{m}}_h|} \right\|_2 \leq \left\| \frac{1}{|\tilde{\mathbf{m}}_h|} \right\|_\infty \cdot \|\nabla_h \tilde{\mathbf{e}}_h\|_2 + \|\tilde{\mathbf{e}}_h\|_2 \cdot \left\| \nabla_h \frac{1}{|\tilde{\mathbf{m}}_h|} \right\|_\infty \leq \mathcal{C}\|\nabla_h \tilde{\mathbf{e}}_h\|_2 + \mathcal{C}\|\tilde{\mathbf{e}}_h\|_2. \tag{2.26}$$

For the second part, we rewrite it as

$$\frac{\underline{\mathbf{m}}_h}{|\underline{\mathbf{m}}_h|} (1 - |\tilde{\mathbf{m}}_h|) = \frac{\underline{\mathbf{m}}_h}{|\underline{\mathbf{m}}_h|} \frac{(\underline{\mathbf{m}}_h + \tilde{\mathbf{m}}_h)(\underline{\mathbf{m}}_h - \tilde{\mathbf{m}}_h)}{1 + |\tilde{\mathbf{m}}_h|} + \frac{\underline{\mathbf{m}}_h}{|\underline{\mathbf{m}}_h|} \frac{(\mathbf{m}_e + \underline{\mathbf{m}}_h)(\mathbf{m}_e - \underline{\mathbf{m}}_h)}{1 + |\tilde{\mathbf{m}}_h|},$$

based on the fact  $|\mathbf{m}_e| \equiv 1$ . For the nonlinear coefficient terms, we observe the following  $\|\cdot\|_\infty$  bounds

$$\begin{aligned} \|\underline{\mathbf{m}}_h\|_\infty &\leq 1 + \frac{1}{2} = \frac{3}{2}, \text{ since } \underline{\mathbf{m}}_h = \mathcal{P}_h \mathbf{m}_e + h^2 \mathbf{m}^{(1)}, |\mathbf{m}_e| \equiv 1, \|\mathbf{m}^{(1)}\|_\infty \leq \mathcal{C}, \\ \left\| \frac{1}{|\tilde{\mathbf{m}}_h|} \right\|_\infty &\leq 2, \text{ since } |\tilde{\mathbf{m}}_h| \geq \frac{1}{2}, \text{ (by (2.18))}, \\ \left\| \frac{\underline{\mathbf{m}}_h}{|\underline{\mathbf{m}}_h|} \right\|_\infty &\leq \|\underline{\mathbf{m}}_h\|_\infty \cdot \left\| \frac{1}{|\underline{\mathbf{m}}_h|} \right\|_\infty \leq 3, \\ \|\nabla_h \underline{\mathbf{m}}_h\|_\infty &\leq \|\nabla_h \mathbf{m}_e\|_\infty + h^2 \|\mathbf{m}^{(1)}\|_\infty \leq \mathcal{C} + 1, \\ \left\| \nabla_h \left( \frac{1}{|\tilde{\mathbf{m}}_h|} \right) \right\|_\infty &\leq \left\| \frac{1}{|\tilde{\mathbf{m}}_h|} \right\|_\infty^2 \cdot \|\nabla_h (|\tilde{\mathbf{m}}_h|)\|_\infty \leq \left\| \frac{1}{|\tilde{\mathbf{m}}_h|} \right\|_\infty^2 \cdot \|\nabla_h \tilde{\mathbf{m}}_h\|_\infty \\ &\leq 2^2 \cdot M, \text{ (by (2.19))}, \\ \left\| \nabla_h \left( \frac{\underline{\mathbf{m}}_h}{|\underline{\mathbf{m}}_h|} \right) \right\|_\infty &\leq \left\| \nabla_h \left( \frac{1}{|\underline{\mathbf{m}}_h|} \right) \right\|_\infty \cdot \|\underline{\mathbf{m}}_h\|_\infty + \left\| \frac{1}{|\underline{\mathbf{m}}_h|} \right\|_\infty \cdot \|\nabla_h \underline{\mathbf{m}}_h\|_\infty \\ &\leq 6M + 2(\mathcal{C} + 1), \end{aligned}$$

$$\begin{aligned} \|\underline{\mathbf{m}}_h + \tilde{\mathbf{m}}_h\|_\infty &\leq \|\underline{\mathbf{m}}_h\|_\infty + \|\tilde{\mathbf{m}}_h\|_\infty \leq M + \frac{3}{2}, \\ \left\| \frac{1}{1 + |\tilde{\mathbf{m}}_h|} \right\|_\infty &\leq 1, \\ \left\| \frac{\underline{\mathbf{m}}_h + \tilde{\mathbf{m}}_h}{1 + |\tilde{\mathbf{m}}_h|} \right\|_\infty &\leq \|\underline{\mathbf{m}}_h + \tilde{\mathbf{m}}_h\|_\infty \cdot \left\| \frac{1}{1 + |\tilde{\mathbf{m}}_h|} \right\|_\infty \leq M + \frac{3}{2}, \\ \|\nabla_h(\underline{\mathbf{m}}_h + \tilde{\mathbf{m}}_h)\|_\infty &\leq \|\nabla_h \underline{\mathbf{m}}_h\|_\infty + \|\tilde{\mathbf{m}}_h\|_\infty \leq \mathcal{C} + M + 1, \\ \left\| \nabla_h \left( \frac{1}{1 + |\tilde{\mathbf{m}}_h|} \right) \right\|_\infty &\leq \left\| \frac{1}{1 + |\tilde{\mathbf{m}}_h|} \right\|_\infty^2 \cdot \|\nabla_h(|\tilde{\mathbf{m}}_h|)\|_\infty \\ &\leq \left\| \frac{1}{1 + |\tilde{\mathbf{m}}_h|} \right\|_\infty^2 \cdot \|\nabla_h \tilde{\mathbf{m}}_h\|_\infty \leq M, \\ \left\| \nabla_h \left( \frac{\underline{\mathbf{m}}_h + \tilde{\mathbf{m}}_h}{1 + |\tilde{\mathbf{m}}_h|} \right) \right\|_\infty &\leq \left\| \nabla_h \left( \frac{1}{1 + |\tilde{\mathbf{m}}_h|} \right) \right\|_\infty \cdot \|\underline{\mathbf{m}}_h + \tilde{\mathbf{m}}_h\|_\infty \\ &\quad + \left\| \frac{1}{1 + |\tilde{\mathbf{m}}_h|} \right\|_\infty \cdot \|\nabla_h(\underline{\mathbf{m}}_h + \tilde{\mathbf{m}}_h)\|_\infty \\ &\leq M(M + \frac{3}{2}) + \mathcal{C} + M + 1. \end{aligned}$$

As a result of these inequalities, we arrive at

$$\begin{aligned} \left\| \frac{\underline{\mathbf{m}}_h}{|\tilde{\mathbf{m}}_h|} \frac{\underline{\mathbf{m}}_h + \tilde{\mathbf{m}}_h}{1 + |\tilde{\mathbf{m}}_h|} \right\|_\infty &\leq \left\| \frac{\underline{\mathbf{m}}_h}{|\tilde{\mathbf{m}}_h|} \right\|_\infty \cdot \left\| \frac{\underline{\mathbf{m}}_h + \tilde{\mathbf{m}}_h}{1 + |\tilde{\mathbf{m}}_h|} \right\|_\infty \leq 3(M + \frac{3}{2}) \leq \mathcal{C}, \\ \left\| \nabla_h \left[ \frac{\underline{\mathbf{m}}_h}{|\tilde{\mathbf{m}}_h|} \frac{\underline{\mathbf{m}}_h + \tilde{\mathbf{m}}_h}{1 + |\tilde{\mathbf{m}}_h|} \right] \right\|_\infty &\leq \left\| \frac{\underline{\mathbf{m}}_h}{|\tilde{\mathbf{m}}_h|} \right\|_\infty \cdot \left\| \nabla_h \left( \frac{\underline{\mathbf{m}}_h + \tilde{\mathbf{m}}_h}{1 + |\tilde{\mathbf{m}}_h|} \right) \right\|_\infty + \left\| \nabla_h \left( \frac{\underline{\mathbf{m}}_h}{|\tilde{\mathbf{m}}_h|} \right) \right\|_\infty \cdot \left\| \frac{\underline{\mathbf{m}}_h + \tilde{\mathbf{m}}_h}{1 + |\tilde{\mathbf{m}}_h|} \right\|_\infty \\ &\leq 3M(M + 3) + 3(\mathcal{C} + 1) + (M + \frac{3}{2})(6M + 2(\mathcal{C} + 1)) \leq \mathcal{C}, \end{aligned}$$

in which  $\mathcal{C}$  has a different value in the last step, which stands for another controllable constant. In turn, the following two estimates could be derived for the two expansion terms:

$$\begin{aligned} &\left\| \nabla_h \left[ \frac{\underline{\mathbf{m}}_h}{|\tilde{\mathbf{m}}_h|} \frac{(\underline{\mathbf{m}}_h + \tilde{\mathbf{m}}_h)(\underline{\mathbf{m}}_h - \tilde{\mathbf{m}}_h)}{1 + |\tilde{\mathbf{m}}_h|} \right] \right\|_2 \\ &\leq \left\| \frac{\underline{\mathbf{m}}_h}{|\tilde{\mathbf{m}}_h|} \frac{\underline{\mathbf{m}}_h + \tilde{\mathbf{m}}_h}{1 + |\tilde{\mathbf{m}}_h|} \right\|_\infty \cdot \|\nabla_h(\underline{\mathbf{m}}_h - \tilde{\mathbf{m}}_h)\|_2 \\ &\quad + \|\underline{\mathbf{m}}_h - \tilde{\mathbf{m}}_h\|_2 \cdot \left\| \nabla_h \left[ \frac{\underline{\mathbf{m}}_h}{|\tilde{\mathbf{m}}_h|} \frac{\underline{\mathbf{m}}_h + \tilde{\mathbf{m}}_h}{1 + |\tilde{\mathbf{m}}_h|} \right] \right\|_\infty \\ &\leq \mathcal{C}\|\nabla_h \tilde{\mathbf{e}}_h\|_2 + \mathcal{C}\|\tilde{\mathbf{e}}_h\|_2, \end{aligned}$$

and

$$\begin{aligned} &\left\| \nabla_h \left[ \frac{\underline{\mathbf{m}}_h}{|\tilde{\mathbf{m}}_h|} \frac{(\underline{\mathbf{m}}_e + \underline{\mathbf{m}}_h)(\underline{\mathbf{m}}_e - \underline{\mathbf{m}}_h)}{1 + |\tilde{\mathbf{m}}_h|} \right] \right\|_2 \\ &\leq \left\| \frac{\underline{\mathbf{m}}_h}{|\tilde{\mathbf{m}}_h|} \frac{\underline{\mathbf{m}}_e + \underline{\mathbf{m}}_h}{1 + |\tilde{\mathbf{m}}_h|} \right\|_\infty \cdot \|\nabla_h(\underline{\mathbf{m}}_e - \underline{\mathbf{m}}_h)\|_2 \\ &\quad + \|\underline{\mathbf{m}}_e - \underline{\mathbf{m}}_h\|_2 \cdot \left\| \nabla_h \left[ \frac{\underline{\mathbf{m}}_h}{|\tilde{\mathbf{m}}_h|} \frac{\underline{\mathbf{m}}_e + \underline{\mathbf{m}}_h}{1 + |\tilde{\mathbf{m}}_h|} \right] \right\|_\infty = \mathcal{O}(h^2). \end{aligned}$$

Therefore, we obtain

$$\left\| \nabla_h \frac{\underline{\mathbf{m}}_h^n}{|\tilde{\mathbf{m}}_h^n|} (1 - |\tilde{\mathbf{m}}_h^n|) \right\|_2 \leq \mathcal{C}(\|\nabla_h \tilde{\mathbf{e}}_h\|_2 + \|\tilde{\mathbf{e}}_h\|_2) + \mathcal{O}(h^2). \tag{2.27}$$

Finally, a substitution of (2.26) and (2.27) into (2.25) yields the second inequality in (2.20). This completes the proof of Lemma 2.5.  $\square$

### 2.4. The unique solvability analysis

To facilitate the unique solvability analysis for (2.11), we denote  $\mathbf{q}_h = -\Delta_h \tilde{\mathbf{m}}_h$ . Note that  $\overline{\mathbf{q}_h} = 0$ , due to the Neumann boundary condition for  $\tilde{\mathbf{m}}_h$ . Meanwhile, we observe that  $\tilde{\mathbf{m}}_h \neq (-\Delta_h)^{-1} \mathbf{q}_h$  in general, since  $\overline{\tilde{\mathbf{m}}_h} \neq 0$ . Instead,  $\tilde{\mathbf{m}}_h$  could be represented as follows:

$$\tilde{\mathbf{m}}_h = (-\Delta_h)^{-1} \mathbf{q}_h + \mathbf{C}_{\mathbf{q}_h}^*, \quad \text{with } \mathbf{C}_{\mathbf{q}_h}^* = \frac{2}{3} \left( \overline{\mathbf{p}_h} + \overline{k \hat{\mathbf{m}}_h \times \mathbf{q}_h} + \alpha \overline{k \hat{\mathbf{m}}_h \times (\hat{\mathbf{m}}_h \times \mathbf{q}_h)} \right),$$

and  $\hat{\mathbf{m}}_h$  given by (2.6). (2.11) is then rewritten as

$$G(\mathbf{q}_h) := \frac{\frac{3}{2} ((-\Delta_h)^{-1} \mathbf{q}_h + \mathbf{C}_{\mathbf{q}_h}^*) - \mathbf{p}_h}{k} - \hat{\mathbf{m}}_h \times \mathbf{q}_h - \alpha \hat{\mathbf{m}}_h \times (\hat{\mathbf{m}}_h \times \mathbf{q}_h) = \mathbf{0}. \tag{2.28}$$

**Lemma 2.6** (Browder-Minty lemma [10,39]). Let  $X$  be a real, reflexive Banach space and let  $T : X \rightarrow X'$  (the dual space of  $X$ ) be bounded, continuous, coercive (i.e.,  $\frac{\langle T(u), u \rangle}{\|u\|_X} \rightarrow +\infty$ , as  $\|u\|_X \rightarrow +\infty$ ) and monotone. Then for any  $g \in X'$  there exists a solution  $u \in X$  of the equation  $T(u) = g$ .

Furthermore, if the operator  $T$  is strictly monotone, then the solution  $u$  is unique.

Then we proceed into the proof of Theorem 2.1.

**Proof.** Recall that (2.11) is equivalent to (2.28). For any  $\mathbf{q}_{1,h}, \mathbf{q}_{2,h}$  with  $\overline{\mathbf{q}_{1,h}} = \overline{\mathbf{q}_{2,h}} = 0$ , we denote  $\tilde{\mathbf{q}}_h = \mathbf{q}_{1,h} - \mathbf{q}_{2,h}$  and derive the following monotonicity estimate:

$$\begin{aligned} & \langle G(\mathbf{q}_{1,h}) - G(\mathbf{q}_{2,h}), \mathbf{q}_{1,h} - \mathbf{q}_{2,h} \rangle \\ &= \frac{3}{2k} \left( \langle (-\Delta_h)^{-1} \tilde{\mathbf{q}}_h, \tilde{\mathbf{q}}_h \rangle + \langle \mathbf{C}_{\mathbf{q}_{1,h}}^* - \mathbf{C}_{\mathbf{q}_{2,h}}^*, \tilde{\mathbf{q}}_h \rangle \right) \\ & \quad - \langle \hat{\mathbf{m}}_h \times \tilde{\mathbf{q}}_h, \tilde{\mathbf{q}}_h \rangle - \alpha \langle \hat{\mathbf{m}}_h \times (\hat{\mathbf{m}}_h \times \tilde{\mathbf{q}}_h), \tilde{\mathbf{q}}_h \rangle \\ & \geq \frac{3}{2k} \left( \langle (-\Delta_h)^{-1} \tilde{\mathbf{q}}_h, \tilde{\mathbf{q}}_h \rangle + \langle \mathbf{C}_{\mathbf{q}_{1,h}}^* - \mathbf{C}_{\mathbf{q}_{2,h}}^*, \tilde{\mathbf{q}}_h \rangle \right) \\ &= \frac{3}{2k} \langle (-\Delta_h)^{-1} \tilde{\mathbf{q}}_h, \tilde{\mathbf{q}}_h \rangle = \frac{3}{2k} \|\tilde{\mathbf{q}}_h\|_{-1}^2 \geq 0. \end{aligned}$$

Note that the following equality and inequality have been applied in the second step:

$$\langle \hat{\mathbf{m}}_h \times \tilde{\mathbf{q}}_h, \tilde{\mathbf{q}}_h \rangle = 0, \quad \langle \hat{\mathbf{m}}_h \times (\hat{\mathbf{m}}_h \times \tilde{\mathbf{q}}_h), \tilde{\mathbf{q}}_h \rangle \leq 0.$$

The third step is based on the fact that both  $\mathbf{C}_{\mathbf{q}_{1,h}}^*$  and  $\mathbf{C}_{\mathbf{q}_{2,h}}^*$  are constants, and  $\overline{\mathbf{q}_{1,h}} = \overline{\mathbf{q}_{2,h}} = 0$ , so that  $\langle \mathbf{C}_{\mathbf{q}_{1,h}}^* - \mathbf{C}_{\mathbf{q}_{2,h}}^*, \tilde{\mathbf{q}}_h \rangle = 0$ . Moreover, for any  $\mathbf{q}_{1,h}, \mathbf{q}_{2,h}$  with  $\overline{\mathbf{q}_{1,h}} = \overline{\mathbf{q}_{2,h}} = 0$ , we get

$$\langle G(\mathbf{q}_{1,h}) - G(\mathbf{q}_{2,h}), \mathbf{q}_{1,h} - \mathbf{q}_{2,h} \rangle \geq \frac{3}{2k} \|\tilde{\mathbf{q}}_h\|_{-1}^2 > 0, \quad \text{if } \mathbf{q}_{1,h} \neq \mathbf{q}_{2,h},$$

and the equality only holds when  $\mathbf{q}_{1,h} = \mathbf{q}_{2,h}$ .

Therefore, an application of Lemma 2.6 implies a unique solution of both (2.28) and (2.11), which completes the proof of Theorem 2.1.  $\square$

### 2.5. The optimal rate convergence analysis: proof of Theorem 2.2

**Proof.** First, we construct an approximate solution  $\underline{\mathbf{m}}$ :

$$\underline{\mathbf{m}} = \mathbf{m}_e + h^2 \mathbf{m}^{(1)}, \tag{2.29}$$

in which the auxiliary field  $\mathbf{m}^{(1)}$  satisfies the following Poisson equation

$$\Delta \mathbf{m}^{(1)} = \hat{\mathbf{C}} \quad \text{with } \hat{\mathbf{C}} = \frac{1}{|\Omega|} \int_{\partial\Omega} \partial_{\mathbf{v}}^3 \mathbf{m}_e \, ds, \tag{2.30}$$

$$\partial_z \mathbf{m}^{(1)}|_{z=0} = -\frac{1}{24} \partial_z^3 \mathbf{m}_e|_{z=0}, \quad \partial_z \mathbf{m}^{(1)}|_{z=1} = \frac{1}{24} \partial_z^3 \mathbf{m}_e|_{z=1},$$

with boundary conditions along  $x$  and  $y$  directions defined in a similar way.

The purpose of such a construction will be illustrated later. Then we extend the approximate profile  $\underline{\mathbf{m}}$  to the numerical “ghost” points, according to the extrapolation formula (2.3):

$$\underline{\mathbf{m}}_{i,j,0} = \underline{\mathbf{m}}_{i,j,1}, \quad \underline{\mathbf{m}}_{i,j,N_z+1} = \underline{\mathbf{m}}_{i,j,N_z}, \tag{2.31}$$

and the extrapolation for other boundaries can be formulated in the same manner. Subsequently, we prove that such an extrapolation yields a higher order  $\mathcal{O}(h^5)$  approximation, instead of the standard  $\mathcal{O}(h^3)$  accuracy. Also see the related works [42,45,46] in the existing literature.

Performing a careful Taylor expansion for the exact solution around the boundary section  $z = 0$ , combined with the mesh point values:  $\hat{z}_0 = -\frac{1}{2}h$ ,  $\hat{z}_1 = \frac{1}{2}h$ , we get

$$\begin{aligned} \mathbf{m}_e(\hat{x}_i, \hat{y}_j, \hat{z}_0) &= \mathbf{m}_e(\hat{x}_i, \hat{y}_j, \hat{z}_1) - h\partial_z \mathbf{m}_e(\hat{x}_i, \hat{y}_j, 0) - \frac{h^3}{24} \partial_z^3 \mathbf{m}_e(\hat{x}_i, \hat{y}_j, 0) + \mathcal{O}(h^5) \\ &= \mathbf{m}_e(\hat{x}_i, \hat{y}_j, \hat{z}_1) - \frac{h^3}{24} \partial_z^3 \mathbf{m}_e(\hat{x}_i, \hat{y}_j, 0) + \mathcal{O}(h^5), \end{aligned} \tag{2.32}$$

in which the homogenous boundary condition has been applied in the second step. A similar Taylor expansion for the constructed profile  $\mathbf{m}^{(1)}$  reveals that

$$\begin{aligned} \mathbf{m}^{(1)}(\hat{x}_i, \hat{y}_j, \hat{z}_0) &= \mathbf{m}^{(1)}(\hat{x}_i, \hat{y}_j, \hat{z}_1) - h\partial_z \mathbf{m}^{(1)}(\hat{x}_i, \hat{y}_j, 0) + \mathcal{O}(h^3) \\ &= \mathbf{m}^{(1)}(\hat{x}_i, \hat{y}_j, \hat{z}_1) + \frac{h}{24} \partial_z^3 \mathbf{m}_e(\hat{x}_i, \hat{y}_j, 0) + \mathcal{O}(h^3) \end{aligned} \tag{2.33}$$

with the boundary condition in (2.30) applied. In turn, a substitution of (2.32)-(2.33) into (2.29) indicates that

$$\underline{\mathbf{m}}(\hat{x}_i, \hat{y}_j, \hat{z}_0) = \underline{\mathbf{m}}(\hat{x}_i, \hat{y}_j, \hat{z}_1) + \mathcal{O}(h^5). \tag{2.34}$$

In other words, the extrapolation formula (2.31) is indeed  $\mathcal{O}(h^5)$  accurate.

As a result of the boundary extrapolation estimate (2.34), we see that the discrete Laplacian of  $\underline{\mathbf{m}}$  yields the second-order accuracy, even at the mesh points around the boundary sections:

$$\Delta_h \underline{\mathbf{m}}_{i,j,k} = \Delta \mathbf{m}_e(\hat{x}_i, \hat{y}_j, \hat{z}_k) + \mathcal{O}(h^2), \quad \forall 1 \leq i, j, k \leq N. \tag{2.35}$$

Moreover, a detailed calculation of Taylor expansion, in both time and space, leads to the following truncation error estimate:

$$\begin{aligned} \frac{\frac{3}{2} \underline{\mathbf{m}}_h^{n+2} - 2 \underline{\mathbf{m}}_h^{n+1} + \frac{1}{2} \underline{\mathbf{m}}_h^n}{k} &= - \left( 2 \underline{\mathbf{m}}_h^{n+1} - \underline{\mathbf{m}}_h^n \right) \times \Delta_h \underline{\mathbf{m}}_h^{n+2} + \tau^{n+2} \\ &\quad - \alpha \left( 2 \underline{\mathbf{m}}_h^{n+1} - \underline{\mathbf{m}}_h^n \right) \times \left( (2 \underline{\mathbf{m}}_h^{n+1} - \underline{\mathbf{m}}_h^n) \times \Delta_h \underline{\mathbf{m}}_h^{n+2} \right), \end{aligned} \tag{2.36}$$

with  $\|\tau^{n+2}\|_2 \leq \mathcal{C}(k^2 + h^2)$ . In addition, a higher order Taylor expansion in space and time reveals the following estimate for the discrete gradient of the truncation error:

$$\|\nabla_h \tau^{n+1}\|_2 \leq \mathcal{C}(k^2 + h^2). \tag{2.37}$$

In fact, such a discrete  $\|\cdot\|_{H_h^1}$  bound for the truncation comes from the regularity assumption for the exact solution,  $\mathbf{m}_e \in C^3([0, T]; C^1) \cap C^1([0, T]; C^3) \cap L^\infty([0, T]; C^5)$ , as stated in Theorem 2.2, as well as the fact that  $\mathbf{m}^{(1)} \in C^1([0, T]; C^1) \cap L^\infty([0, T]; C^2)$ , as indicated by the Poisson equation (2.30).

In turn, we introduce the numerical error functions  $\tilde{\mathbf{e}}_h^n = \underline{\mathbf{m}}_h^n - \tilde{\mathbf{m}}_h^n$ ,  $\mathbf{e}_h^n = \underline{\mathbf{m}}_h^n - \mathbf{m}_h^n$ , at a point-wise level. In other words, instead of a direct comparison between the numerical solution and the exact solution, we analyze the error function between the numerical solution and the constructed solution  $\underline{\mathbf{m}}_h$ , due to its higher order consistency estimate (2.34) around the boundary. A subtraction of (2.7)-(2.8) from the consistency estimate (2.36) leads to the error function evolution system:

$$\begin{aligned} \frac{\frac{3}{2} \tilde{\mathbf{e}}_h^{n+2} - 2 \tilde{\mathbf{e}}_h^{n+1} + \frac{1}{2} \tilde{\mathbf{e}}_h^n}{k} &= - \left( 2 \underline{\mathbf{m}}_h^{n+1} - \underline{\mathbf{m}}_h^n \right) \times \Delta_h \tilde{\mathbf{e}}_h^{n+2} - \left( 2 \mathbf{e}_h^{n+1} - \mathbf{e}_h^n \right) \times \Delta_h \underline{\mathbf{m}}_h^{n+2} \\ &\quad - \alpha \left( 2 \underline{\mathbf{m}}_h^{n+1} - \underline{\mathbf{m}}_h^n \right) \times \left( (2 \underline{\mathbf{m}}_h^{n+1} - \underline{\mathbf{m}}_h^n) \times \Delta_h \tilde{\mathbf{e}}_h^{n+2} \right) \\ &\quad - \alpha \left( 2 \underline{\mathbf{m}}_h^{n+1} - \underline{\mathbf{m}}_h^n \right) \times \left( (2 \mathbf{e}_h^{n+1} - \mathbf{e}_h^n) \times \Delta_h \underline{\mathbf{m}}_h^{n+2} \right) \\ &\quad - \alpha \left( 2 \mathbf{e}_h^{n+1} - \mathbf{e}_h^n \right) \times \left( (2 \underline{\mathbf{m}}_h^{n+1} - \underline{\mathbf{m}}_h^n) \times \Delta_h \underline{\mathbf{m}}_h^{n+2} \right) + \tau^{n+2}. \end{aligned} \tag{2.38}$$

Before we proceed into the formal error estimate, we establish the bound for the constructed approximate solution  $\underline{\mathbf{m}}$  and the numerical solution  $\mathbf{m}_h$ . For the approximate profile  $\underline{\mathbf{m}} \in L^\infty([0, T], C^5)$ , which turns out to be the exact solution and an  $\mathcal{O}(h^2)$  correction term, we still use  $\mathcal{C}$  to denote its bound:

$$\|\nabla_h^r \underline{\mathbf{m}}_h\|_\infty \leq \mathcal{C}, \quad r = 0, 1, 2, 3, \tag{2.39}$$

in which  $\underline{\mathbf{m}}_h = \mathcal{P}_h \underline{\mathbf{m}}$ , the point-wise interpolation of the constructed continuous function  $\underline{\mathbf{m}}$ . In addition, we make the following *a priori* assumption for the numerical error function:

$$\|\mathbf{e}_h^k\|_\infty + \|\nabla_h \mathbf{e}_h^k\|_\infty \leq \frac{1}{3}, \quad \|\tilde{\mathbf{e}}_h^k\|_\infty + \|\nabla_h \tilde{\mathbf{e}}_h^k\|_\infty \leq \frac{1}{3}, \quad \text{for } k = \ell, \ell + 1. \tag{2.40}$$

Such an assumption will be recovered by the convergence analysis at time step  $t^{\ell+2}$ . In turn, an application of triangle inequality yields the desired  $W_h^{1,\infty}$  bound for the numerical solutions  $\mathbf{m}_h$  and  $\tilde{\mathbf{m}}_h$ :

$$\|\mathbf{m}_h^k\|_\infty = \|\underline{\mathbf{m}}_h^k - \mathbf{e}_h^k\|_\infty \leq \|\underline{\mathbf{m}}_h^k\|_\infty + \|\mathbf{e}_h^k\|_\infty \leq \mathcal{C} + \frac{1}{3}, \tag{2.41}$$

$$\|\nabla_h \mathbf{m}_h^k\|_\infty = \|\nabla_h \underline{\mathbf{m}}_h^k - \nabla_h \mathbf{e}_h^k\|_\infty \leq \|\nabla_h \underline{\mathbf{m}}_h^k\|_\infty + \|\nabla_h \mathbf{e}_h^k\|_\infty \leq \mathcal{C} + \frac{1}{3},$$

$$\|\tilde{\mathbf{m}}_h^k\|_\infty \leq \mathcal{C} + \frac{1}{3}, \quad \|\nabla_h \tilde{\mathbf{m}}_h^k\|_\infty \leq \mathcal{C} + \frac{1}{3} \quad (\text{similar derivation}). \tag{2.42}$$

Then we perform a discrete  $L^2$  error estimate at  $t^{\ell+2}$  using the mathematical induction. By taking a discrete inner product with the numerical error equation (2.38) by  $\tilde{\mathbf{e}}_h^{\ell+2}$  gives that

$$\begin{aligned} R.H.S. &= \left\langle -\left(2\mathbf{m}_h^{\ell+1} - \mathbf{m}_h^\ell\right) \times \Delta_h \tilde{\mathbf{e}}_h^{\ell+2}, \tilde{\mathbf{e}}_h^{\ell+2} \right\rangle \\ &\quad - \left\langle \left(2\mathbf{e}_h^{\ell+1} - \mathbf{e}_h^\ell\right) \times \Delta_h \underline{\mathbf{m}}_h^{\ell+2}, \tilde{\mathbf{e}}_h^{\ell+2} \right\rangle + \left\langle \tau^{\ell+2}, \tilde{\mathbf{e}}_h^{\ell+2} \right\rangle \\ &\quad - \alpha \left\langle \left(2\mathbf{m}_h^{\ell+1} - \mathbf{m}_h^\ell\right) \times \left(2\mathbf{m}_h^{\ell+1} - \mathbf{m}_h^\ell\right) \times \Delta_h \tilde{\mathbf{e}}_h^{\ell+2}, \tilde{\mathbf{e}}_h^{\ell+2} \right\rangle \\ &\quad - \alpha \left\langle \left(2\mathbf{m}_h^{\ell+1} - \mathbf{m}_h^\ell\right) \times \left(2\mathbf{e}_h^{\ell+1} - \mathbf{e}_h^\ell\right) \times \Delta_h \underline{\mathbf{m}}_h^{\ell+2}, \tilde{\mathbf{e}}_h^{\ell+2} \right\rangle \\ &\quad - \alpha \left\langle \left(2\mathbf{e}_h^{\ell+1} - \mathbf{e}_h^\ell\right) \times \left(2\mathbf{m}_h^{\ell+1} - \mathbf{m}_h^\ell\right) \times \Delta_h \underline{\mathbf{m}}_h^{\ell+2}, \tilde{\mathbf{e}}_h^{\ell+2} \right\rangle \\ &=: \tilde{I}_1 + \tilde{I}_2 + \tilde{I}_3 + \tilde{I}_4 + \tilde{I}_5 + \tilde{I}_6. \end{aligned} \tag{2.43}$$

- Estimate of  $\tilde{I}_1$ : A combination of the summation by parts formula (2.13) (notice that the numerical error function  $\tilde{\mathbf{e}}$  satisfies the homogeneous Neumann boundary condition (2.3)) and inequality (2.14) results in

$$\begin{aligned} \tilde{I}_1 &= \left\langle -\left(2\mathbf{m}_h^{\ell+1} - \mathbf{m}_h^\ell\right) \times \Delta_h \tilde{\mathbf{e}}_h^{\ell+2}, \tilde{\mathbf{e}}_h^{\ell+2} \right\rangle \\ &= \left\langle \tilde{\mathbf{e}}_h^{\ell+2} \times \left(2\mathbf{m}_h^{\ell+1} - \mathbf{m}_h^\ell\right), -\Delta_h \tilde{\mathbf{e}}_h^{\ell+2} \right\rangle \\ &= \left\langle \nabla_h \left[ \tilde{\mathbf{e}}_h^{\ell+2} \times \left(2\mathbf{m}_h^{\ell+1} - \mathbf{m}_h^\ell\right) \right], \nabla_h \tilde{\mathbf{e}}_h^{\ell+2} \right\rangle \\ &\leq \mathcal{C} \left( \|\nabla_h \tilde{\mathbf{e}}_h^{\ell+2}\|_2^2 + \|\nabla_h \tilde{\mathbf{e}}_h^{\ell+2}\|_2^2 \cdot \|2\mathbf{m}_h^{\ell+1} - \mathbf{m}_h^\ell\|_\infty^2 \right. \\ &\quad \left. + \|\tilde{\mathbf{e}}_h^{\ell+2}\|_2^2 \cdot \|\nabla_h (2\mathbf{m}_h^{\ell+1} - \mathbf{m}_h^\ell)\|_\infty^2 \right) \\ &\leq \mathcal{C} (\|\nabla_h \tilde{\mathbf{e}}_h^{\ell+2}\|_2^2 + \|\tilde{\mathbf{e}}_h^{\ell+2}\|_2^2). \end{aligned} \tag{2.44}$$

- Estimate of  $\tilde{I}_2$ :

$$\begin{aligned} \tilde{I}_2 &= -\left\langle \left(2\mathbf{e}_h^{\ell+1} - \mathbf{e}_h^\ell\right) \times \Delta_h \underline{\mathbf{m}}_h^{\ell+2}, \tilde{\mathbf{e}}_h^{\ell+2} \right\rangle \\ &\leq \frac{1}{2} \left[ \|\tilde{\mathbf{e}}_h^{\ell+2}\|_2^2 + \|2\mathbf{e}_h^{\ell+1} - \mathbf{e}_h^\ell\|_2^2 \cdot \|\Delta_h \underline{\mathbf{m}}_h^{\ell+2}\|_\infty^2 \right] \\ &\leq \mathcal{C} (\|\tilde{\mathbf{e}}_h^{\ell+2}\|_2^2 + \|\mathbf{e}_h^{\ell+1}\|_2^2 + \|\mathbf{e}_h^\ell\|_2^2), \end{aligned} \tag{2.45}$$

in which the bound for  $\|\Delta_h \underline{\mathbf{m}}_h^{\ell+2}\|_\infty$  is given by the preliminary estimate (2.39), with  $r = 2$ .

- Estimate of the truncation error term  $\tilde{I}_3$ : An application of Cauchy inequality gives

$$\tilde{I}_3 = \left\langle \tau^{\ell+2}, \tilde{\mathbf{e}}_h^{\ell+2} \right\rangle \leq C \|\tilde{\mathbf{e}}_h^{\ell+2}\|_2^2 + C(k^4 + h^4). \tag{2.46}$$

- Estimate of  $\tilde{I}_4$ : It follows from (2.15) in Lemma 2.4 that

$$\begin{aligned} \tilde{I}_4 &= -\alpha \left\langle \left(2\mathbf{m}_h^{\ell+1} - \mathbf{m}_h^\ell\right) \times \left(2\mathbf{m}_h^{\ell+1} - \mathbf{m}_h^\ell\right) \times \Delta_h \tilde{\mathbf{e}}_h^{\ell+2}, \tilde{\mathbf{e}}_h^{\ell+2} \right\rangle \\ &= \alpha \left\langle \left(2\mathbf{m}_h^{\ell+1} - \mathbf{m}_h^\ell\right) \times \Delta_h \tilde{\mathbf{e}}_h^{\ell+2} \right\rangle \times \left(2\mathbf{m}_h^{\ell+1} - \mathbf{m}_h^\ell\right), \tilde{\mathbf{e}}_h^{\ell+2} \rangle \\ &= \alpha \left\langle \left(2\mathbf{m}_h^{\ell+1} - \mathbf{m}_h^\ell\right) \times \left[\tilde{\mathbf{e}}_h^{\ell+2} \times \left(2\mathbf{m}_h^{\ell+1} - \mathbf{m}_h^\ell\right)\right], \Delta_h \tilde{\mathbf{e}}_h^{\ell+2} \right\rangle \\ &= \alpha \left\langle \nabla_h \left( \left(2\mathbf{m}_h^{\ell+1} - \mathbf{m}_h^\ell\right) \times \left[\tilde{\mathbf{e}}_h^{\ell+2} \times \left(2\mathbf{m}_h^{\ell+1} - \mathbf{m}_h^\ell\right)\right] \right), \nabla_h \tilde{\mathbf{e}}_h^{\ell+2} \right\rangle \\ &\leq C \left( \|\nabla_h \tilde{\mathbf{e}}_h^{\ell+2}\|_2^2 + \|\nabla_h (2\mathbf{m}_h^{\ell+1} - \mathbf{m}_h^\ell)\|_\infty^2 \cdot \|\tilde{\mathbf{e}}_h^{\ell+2}\|_2^2 \cdot \|2\mathbf{m}_h^{\ell+1} - \mathbf{m}_h^\ell\|_\infty^2 \right. \\ &\quad \left. + \|2\mathbf{m}_h^{\ell+1} - \mathbf{m}_h^\ell\|_\infty^2 \cdot \|\nabla_h \tilde{\mathbf{e}}_h^{\ell+2}\|_2^2 \cdot \|2\mathbf{m}_h^{\ell+1} - \mathbf{m}_h^\ell\|_\infty^2 \right. \\ &\quad \left. + \|2\mathbf{m}_h^{\ell+1} - \mathbf{m}_h^\ell\|_\infty^2 \cdot \|\tilde{\mathbf{e}}_h^{\ell+2}\|_2^2 \cdot \|\nabla_h (2\mathbf{m}_h^{\ell+1} - \mathbf{m}_h^\ell)\|_\infty^2 \right) \\ &\leq C(\|\nabla_h \tilde{\mathbf{e}}_h^{\ell+2}\|_2^2 + \|\tilde{\mathbf{e}}_h^{\ell+2}\|_2^2). \end{aligned} \tag{2.47}$$

- Estimates of  $\tilde{I}_5$  and  $\tilde{I}_6$ :

$$\begin{aligned} \tilde{I}_5 &= -\alpha \left\langle \left(2\mathbf{m}_h^{\ell+1} - \mathbf{m}_h^\ell\right) \times \left(2\mathbf{e}_h^{\ell+1} - \mathbf{e}_h^\ell\right) \times \Delta_h \underline{\mathbf{m}}_h^{\ell+2}, \tilde{\mathbf{e}}_h^{\ell+2} \right\rangle \\ &\leq \frac{\alpha}{2} \left( \|\tilde{\mathbf{e}}_h^{\ell+2}\|_2^2 + \|2\mathbf{m}_h^{\ell+1} - \mathbf{m}_h^\ell\|_\infty^2 \cdot \|2\mathbf{e}_h^{\ell+1} - \mathbf{e}_h^\ell\|_2^2 \cdot \|\Delta_h \underline{\mathbf{m}}_h^{\ell+2}\|_\infty^2 \right) \\ &\leq C(\|\tilde{\mathbf{e}}_h^{\ell+2}\|_2^2 + \|\mathbf{e}_h^{\ell+1}\|_2^2 + \|\mathbf{e}_h^\ell\|_2^2). \end{aligned} \tag{2.48}$$

$$\begin{aligned} \tilde{I}_6 &= -\alpha \left\langle \left(2\mathbf{e}_h^{\ell+1} - \mathbf{e}_h^\ell\right) \times \left(2\underline{\mathbf{m}}_h^{\ell+1} - \underline{\mathbf{m}}_h^\ell\right) \times \Delta_h \underline{\mathbf{m}}_h^{\ell+2}, \tilde{\mathbf{e}}_h^{\ell+2} \right\rangle \\ &\leq \frac{\alpha}{2} \left( \|\tilde{\mathbf{e}}_h^{\ell+2}\|_2^2 + \|2\mathbf{e}_h^{\ell+1} - \mathbf{e}_h^\ell\|_2^2 \cdot \|2\underline{\mathbf{m}}_h^{\ell+1} - \underline{\mathbf{m}}_h^\ell\|_\infty^2 \cdot \|\Delta_h \underline{\mathbf{m}}_h^{\ell+2}\|_\infty^2 \right) \\ &\leq C(\|\tilde{\mathbf{e}}_h^{\ell+2}\|_2^2 + \|\mathbf{e}_h^{\ell+1}\|_2^2 + \|\mathbf{e}_h^\ell\|_2^2). \end{aligned} \tag{2.49}$$

Again, the bound for  $\|\Delta_h \underline{\mathbf{m}}_h^{\ell+2}\|_\infty$  is given by the preliminary estimate (2.39), with  $r = 2$ .

Meanwhile, the inner product of the left hand side of (2.38) with  $\tilde{\mathbf{e}}_h^{\ell+2}$  turns out to be

$$\begin{aligned} L.H.S. &= \frac{1}{4k} (\|\tilde{\mathbf{e}}_h^{\ell+2}\|_2^2 - \|\tilde{\mathbf{e}}_h^{\ell+1}\|_2^2 + \|2\tilde{\mathbf{e}}_h^{\ell+2} - \tilde{\mathbf{e}}_h^{\ell+1}\|_2^2 - \|2\tilde{\mathbf{e}}_h^{\ell+1} - \tilde{\mathbf{e}}_h^\ell\|_2^2 \\ &\quad + \|\tilde{\mathbf{e}}_h^{\ell+2} - 2\tilde{\mathbf{e}}_h^{\ell+1} + \tilde{\mathbf{e}}_h^\ell\|_2^2). \end{aligned}$$

Its combination with eqs. (2.44) to (2.49) and (2.43) leads to

$$\begin{aligned} &\|\tilde{\mathbf{e}}_h^{\ell+2}\|_2^2 - \|\tilde{\mathbf{e}}_h^{\ell+1}\|_2^2 + \|2\tilde{\mathbf{e}}_h^{\ell+2} - \tilde{\mathbf{e}}_h^{\ell+1}\|_2^2 - \|2\tilde{\mathbf{e}}_h^{\ell+1} - \tilde{\mathbf{e}}_h^\ell\|_2^2 \\ &\leq Ck(\|\nabla_h \tilde{\mathbf{e}}_h^{\ell+2}\|_2^2 + \|\tilde{\mathbf{e}}_h^{\ell+2}\|_2^2 + \|\mathbf{e}_h^{\ell+1}\|_2^2 + \|\mathbf{e}_h^\ell\|_2^2) + Ck(k^4 + h^4). \end{aligned} \tag{2.50}$$

However, the standard  $L^2$  error estimate (2.50) does not allow one to apply discrete Gronwall inequality, due to the  $H_h^1$  norms of the error function involved on the right hand side. To overcome this difficulty, we take a discrete inner product with the numerical error equation (2.38) by  $-\Delta_h \tilde{\mathbf{e}}_h^{\ell+2}$  and see that

$$\begin{aligned} R.H.S. &= \left\langle - \left(2\mathbf{m}_h^{\ell+1} - \mathbf{m}_h^\ell\right) \times \Delta_h \tilde{\mathbf{e}}_h^{\ell+2}, -\Delta_h \tilde{\mathbf{e}}_h^{\ell+2} \right\rangle \\ &\quad - \left\langle \left(2\mathbf{e}_h^{\ell+1} - \mathbf{e}_h^\ell\right) \times \Delta_h \underline{\mathbf{m}}_h^{\ell+2}, -\Delta_h \tilde{\mathbf{e}}_h^{\ell+2} \right\rangle + \left\langle \tau_h^{\ell+2}, -\Delta_h \tilde{\mathbf{e}}_h^{\ell+2} \right\rangle \\ &\quad - \alpha \left\langle \left(2\mathbf{m}_h^{\ell+1} - \mathbf{m}_h^\ell\right) \times \left(2\mathbf{m}_h^{\ell+1} - \mathbf{m}_h^\ell\right) \times \Delta_h \tilde{\mathbf{e}}_h^{\ell+2}, -\Delta_h \tilde{\mathbf{e}}_h^{\ell+2} \right\rangle \\ &\quad - \alpha \left\langle \left(2\mathbf{m}_h^{\ell+1} - \mathbf{m}_h^\ell\right) \times \left(2\mathbf{e}_h^{\ell+1} - \mathbf{e}_h^\ell\right) \times \Delta_h \underline{\mathbf{m}}_h^{\ell+2}, -\Delta_h \tilde{\mathbf{e}}_h^{\ell+2} \right\rangle \\ &\quad - \alpha \left\langle \left(2\mathbf{e}_h^{\ell+1} - \mathbf{e}_h^\ell\right) \times \left(2\underline{\mathbf{m}}_h^{\ell+1} - \underline{\mathbf{m}}_h^\ell\right) \times \Delta_h \underline{\mathbf{m}}_h^{\ell+2}, -\Delta_h \tilde{\mathbf{e}}_h^{\ell+2} \right\rangle \\ &=: I_1 + I_2 + I_3 + I_4 + I_5 + I_6. \end{aligned} \tag{2.51}$$

- Estimate of  $I_1$ :

$$I_1 = \left\langle -(2\mathbf{m}_h^{\ell+1} - \mathbf{m}_h^\ell) \times \Delta_h \tilde{\mathbf{e}}_h^{\ell+2}, -\Delta_h \tilde{\mathbf{e}}_h^{\ell+2} \right\rangle = 0. \tag{2.52}$$

- Estimate of  $I_2$ :

$$\begin{aligned} I_2 &= -\left\langle (2\mathbf{e}_h^{\ell+1} - \mathbf{e}_h^\ell) \times \Delta_h \underline{\mathbf{m}}_h^{\ell+2}, -\Delta_h \tilde{\mathbf{e}}_h^{\ell+2} \right\rangle \\ &= \left\langle \nabla_h \left( \Delta_h \underline{\mathbf{m}}_h^{\ell+2} \times (2\mathbf{e}_h^{\ell+1} - \mathbf{e}_h^\ell) \right), \nabla_h \tilde{\mathbf{e}}_h^{\ell+2} \right\rangle \\ &\leq C \left( \|\nabla_h \tilde{\mathbf{e}}_h^{\ell+2}\|_2^2 + \|\Delta_h \underline{\mathbf{m}}_h^{\ell+2}\|_\infty^2 \cdot \|\nabla_h (2\mathbf{e}_h^{\ell+1} - \mathbf{e}_h^\ell)\|_2^2 \right. \\ &\quad \left. + \|\nabla_h (\Delta_h \underline{\mathbf{m}}_h^{\ell+2})\|_\infty^2 \cdot \|2\mathbf{e}_h^{\ell+1} - \mathbf{e}_h^\ell\|_2^2 \right) \\ &\leq C \left( \|\nabla_h \tilde{\mathbf{e}}_h^{\ell+2}\|_2^2 + \|\nabla_h \mathbf{e}_h^{\ell+1}\|_2^2 + \|\nabla_h \mathbf{e}_h^\ell\|_2^2 + \|\mathbf{e}_h^{\ell+1}\|_2^2 + \|\mathbf{e}_h^\ell\|_2^2 \right). \end{aligned} \tag{2.53}$$

Similarly, the bound for  $\|\nabla_h \Delta_h \underline{\mathbf{m}}_h^{\ell+2}\|_\infty$  comes from the preliminary estimate (2.39), by taking  $r = 3$ .

- Estimate of the truncation error term  $I_3$ :

$$I_3 = \left\langle -\Delta_h \tilde{\mathbf{e}}_h^{\ell+2}, \tau^{\ell+2} \right\rangle \leq C \|\nabla_h \tilde{\mathbf{e}}_h^{\ell+2}\|_2^2 + C(k^4 + h^4), \tag{2.54}$$

in which the discrete  $H_h^1$  estimate (2.37) for the local truncation error has been recalled.

- Estimate of  $I_4$ : It follows from Lemma 2.16 in Lemma 2.4 that

$$\begin{aligned} I_4 &= -\alpha \left\langle (2\mathbf{m}_h^{\ell+1} - \mathbf{m}_h^\ell) \times ((2\mathbf{m}_h^{\ell+1} - \mathbf{m}_h^\ell) \times \Delta_h \tilde{\mathbf{e}}_h^{\ell+2}), -\Delta_h \tilde{\mathbf{e}}_h^{\ell+2} \right\rangle \\ &= \alpha \left\langle (2\mathbf{m}_h^{\ell+1} - \mathbf{m}_h^\ell) \times \Delta_h \tilde{\mathbf{e}}_h^{\ell+2}, \Delta_h \tilde{\mathbf{e}}_h^{\ell+2} \times (2\mathbf{m}_h^{\ell+1} - \mathbf{m}_h^\ell) \right\rangle \\ &= -\alpha \|(2\mathbf{m}_h^{\ell+1} - \mathbf{m}_h^\ell) \times \Delta_h \tilde{\mathbf{e}}_h^{\ell+2}\|_2^2 \leq 0. \end{aligned} \tag{2.55}$$

- Estimates of  $I_5$  and  $I_6$ :

$$\begin{aligned} I_5 &= -\alpha \left\langle (2\mathbf{m}_h^{\ell+1} - \mathbf{m}_h^\ell) \times ((2\mathbf{e}_h^{\ell+1} - \mathbf{e}_h^\ell) \times \Delta_h \underline{\mathbf{m}}_h^{\ell+2}), -\Delta_h \tilde{\mathbf{e}}_h^{\ell+2} \right\rangle \\ &= -\alpha \left\langle \nabla_h \left( (2\mathbf{m}_h^{\ell+1} - \mathbf{m}_h^\ell) \times ((2\mathbf{e}_h^{\ell+1} - \mathbf{e}_h^\ell) \times \Delta_h \underline{\mathbf{m}}_h^{\ell+2}) \right), \nabla_h \tilde{\mathbf{e}}_h^{\ell+2} \right\rangle \\ &\leq C \left( \|\nabla_h \tilde{\mathbf{e}}_h^{\ell+2}\|_2^2 + \|\nabla_h (2\mathbf{m}_h^{\ell+1} - \mathbf{m}_h^\ell)\|_\infty^2 \cdot \|\Delta_h \underline{\mathbf{m}}_h^{\ell+2}\|_\infty^2 \cdot \|2\mathbf{e}_h^{\ell+1} - \mathbf{e}_h^\ell\|_2^2 \right. \\ &\quad \left. + \|2\mathbf{m}_h^{\ell+1} - \mathbf{m}_h^\ell\|_\infty^2 \cdot \|\nabla_h (\Delta_h \underline{\mathbf{m}}_h^{\ell+2})\|_\infty^2 \cdot \|2\mathbf{e}_h^{\ell+1} - \mathbf{e}_h^\ell\|_2^2 \right. \\ &\quad \left. + \|2\mathbf{m}_h^{\ell+1} - \mathbf{m}_h^\ell\|_\infty^2 \cdot \|\Delta_h \underline{\mathbf{m}}_h^{\ell+2}\|_\infty^2 \cdot \|\nabla_h (2\mathbf{e}_h^{\ell+1} - \mathbf{e}_h^\ell)\|_2^2 \right) \\ &\leq C \left( \|\nabla_h \tilde{\mathbf{e}}_h^{\ell+2}\|_2^2 + \|\nabla_h \mathbf{e}_h^{\ell+1}\|_2^2 + \|\nabla_h \mathbf{e}_h^\ell\|_2^2 + \|\mathbf{e}_h^{\ell+1}\|_2^2 + \|\mathbf{e}_h^\ell\|_2^2 \right). \end{aligned} \tag{2.56}$$

$$\begin{aligned} I_6 &= -\alpha \left\langle (2\mathbf{e}_h^{\ell+1} - \mathbf{e}_h^\ell) \times ((2\underline{\mathbf{m}}_h^{\ell+1} - \underline{\mathbf{m}}_h^\ell) \times \Delta_h \underline{\mathbf{m}}_h^{\ell+2}), -\Delta_h \tilde{\mathbf{e}}_h^{\ell+2} \right\rangle \\ &= -\alpha \left\langle \nabla_h \left[ (2\mathbf{e}_h^{\ell+1} - \mathbf{e}_h^\ell) \times ((2\underline{\mathbf{m}}_h^{\ell+1} - \underline{\mathbf{m}}_h^\ell) \times \Delta_h \underline{\mathbf{m}}_h^{\ell+2}) \right], \nabla_h \tilde{\mathbf{e}}_h^{\ell+2} \right\rangle \\ &\leq C \left( \|\nabla_h \tilde{\mathbf{e}}_h^{\ell+2}\|_2^2 + \|\nabla_h (2\mathbf{e}_h^{\ell+1} - \mathbf{e}_h^\ell)\|_2^2 \cdot \|2\underline{\mathbf{m}}_h^{\ell+1} - \underline{\mathbf{m}}_h^\ell\|_\infty^2 \cdot \|\Delta_h \underline{\mathbf{m}}_h^{\ell+2}\|_\infty^2 \right. \\ &\quad \left. + \|2\mathbf{e}_h^{\ell+1} - \mathbf{e}_h^\ell\|_2^2 \cdot \|\nabla_h (2\underline{\mathbf{m}}_h^{\ell+1} - \underline{\mathbf{m}}_h^\ell)\|_\infty^2 \cdot \|\Delta_h \underline{\mathbf{m}}_h^{\ell+2}\|_\infty^2 \right. \\ &\quad \left. + \|2\mathbf{e}_h^{\ell+1} - \mathbf{e}_h^\ell\|_2^2 \cdot \|2\underline{\mathbf{m}}_h^{\ell+1} - \underline{\mathbf{m}}_h^\ell\|_\infty^2 \cdot \|\nabla_h (\Delta_h \underline{\mathbf{m}}_h^{\ell+2})\|_\infty^2 \right) \\ &\leq C \left( \|\nabla_h \tilde{\mathbf{e}}_h^{\ell+2}\|_2^2 + \|\nabla_h \mathbf{e}_h^{\ell+1}\|_2^2 + \|\nabla_h \mathbf{e}_h^\ell\|_2^2 + \|\mathbf{e}_h^{\ell+1}\|_2^2 + \|\mathbf{e}_h^\ell\|_2^2 \right). \end{aligned} \tag{2.57}$$

Again, the bound for  $\|\nabla_h \Delta_h \underline{\mathbf{m}}_h^{\ell+2}\|_\infty$  comes from the preliminary estimate (2.39), by taking  $r = 3$ .

And also, the inner product on the left hand side becomes

$$\begin{aligned} L.H.S. &= \frac{1}{4k} \left( \|\nabla_h \tilde{\mathbf{e}}_h^{\ell+2}\|_2^2 - \|\nabla_h \tilde{\mathbf{e}}_h^{\ell+1}\|_2^2 + \|2\nabla_h \tilde{\mathbf{e}}_h^{\ell+2} - \nabla_h \tilde{\mathbf{e}}_h^{\ell+1}\|_2^2 \right. \\ &\quad \left. - \|2\nabla_h \tilde{\mathbf{e}}_h^{\ell+1} - \nabla_h \tilde{\mathbf{e}}_h^\ell\|_2^2 + \|\nabla_h \tilde{\mathbf{e}}_h^{\ell+2} - 2\nabla_h \tilde{\mathbf{e}}_h^{\ell+1} + \nabla_h \tilde{\mathbf{e}}_h^\ell\|_2^2 \right). \end{aligned} \tag{2.58}$$

Substituting (2.52), eqs. (2.53) to (2.57) into (2.38), combined with (2.58), we arrive at

$$\begin{aligned} & \|\nabla_h \tilde{\mathbf{e}}_h^{\ell+2}\|_2^2 - \|\nabla_h \tilde{\mathbf{e}}_h^{\ell+1}\|_2^2 + \|2\nabla_h \tilde{\mathbf{e}}_h^{\ell+2} - \nabla_h \tilde{\mathbf{e}}_h^{\ell+1}\|_2^2 - \|2\nabla_h \tilde{\mathbf{e}}_h^{\ell+1} - \nabla_h \tilde{\mathbf{e}}_h^\ell\|_2^2 \\ & \leq Ck \left( \|\nabla_h \tilde{\mathbf{e}}_h^{\ell+2}\|_2^2 + \|\nabla_h \tilde{\mathbf{e}}_h^{\ell+1}\|_2^2 + \|\nabla_h \mathbf{e}_h^\ell\|_2^2 + \|\mathbf{e}_h^{\ell+1}\|_2^2 + \|\mathbf{e}_h^\ell\|_2^2 \right) + Ck(k^4 + h^4). \end{aligned} \tag{2.59}$$

As a consequence, a combination of (2.50) and (2.59) yields

$$\begin{aligned} & \|\tilde{\mathbf{e}}_h^{\ell+2}\|_2^2 - \|\tilde{\mathbf{e}}_h^{\ell+1}\|_2^2 + \|2\tilde{\mathbf{e}}_h^{\ell+2} - \tilde{\mathbf{e}}_h^{\ell+1}\|_2^2 - \|2\tilde{\mathbf{e}}_h^{\ell+1} - \tilde{\mathbf{e}}_h^\ell\|_2^2 \\ & + \|\nabla_h \tilde{\mathbf{e}}_h^{\ell+2}\|_2^2 - \|\nabla_h \tilde{\mathbf{e}}_h^{\ell+1}\|_2^2 + \|\nabla_h (2\tilde{\mathbf{e}}_h^{\ell+2} - \tilde{\mathbf{e}}_h^{\ell+1})\|_2^2 - \|\nabla_h (2\tilde{\mathbf{e}}_h^{\ell+1} - \tilde{\mathbf{e}}_h^\ell)\|_2^2 \\ & \leq Ck \left( \|\nabla_h \tilde{\mathbf{e}}_h^{\ell+2}\|_2^2 + \|\tilde{\mathbf{e}}_h^{\ell+2}\|_2^2 + \|\nabla_h \mathbf{e}_h^{\ell+1}\|_2^2 + \|\nabla_h \mathbf{e}_h^\ell\|_2^2 + \|\mathbf{e}_h^{\ell+1}\|_2^2 + \|\mathbf{e}_h^\ell\|_2^2 \right) \\ & + Ck(k^4 + h^4). \end{aligned} \tag{2.60}$$

At this point, recalling the  $W_h^{1,\infty}$  bound for  $\mathbf{m}_h^k$  and  $\tilde{\mathbf{m}}_h^k$ , as given by (2.41), (2.42), and applying (2.20) in Lemma 2.5, we obtain

$$\|\mathbf{e}_h^k\|_2 \leq 2\|\tilde{\mathbf{e}}_h^k\|_2 + \mathcal{O}(h^2), \quad \|\nabla_h \mathbf{e}_h^k\|_2 \leq C(\|\nabla_h \tilde{\mathbf{e}}_h^k\|_2 + \|\tilde{\mathbf{e}}_h^k\|_2) + \mathcal{O}(h^2), \quad k = \ell, \ell + 1.$$

Its substitution into (2.60) leads to

$$\begin{aligned} & \|\tilde{\mathbf{e}}_h^{\ell+2}\|_2^2 - \|\tilde{\mathbf{e}}_h^{\ell+1}\|_2^2 + \|2\tilde{\mathbf{e}}_h^{\ell+2} - \tilde{\mathbf{e}}_h^{\ell+1}\|_2^2 - \|2\tilde{\mathbf{e}}_h^{\ell+1} - \tilde{\mathbf{e}}_h^\ell\|_2^2 \\ & + \|\nabla_h \tilde{\mathbf{e}}_h^{\ell+2}\|_2^2 - \|\nabla_h \tilde{\mathbf{e}}_h^{\ell+1}\|_2^2 + \|\nabla_h (2\tilde{\mathbf{e}}_h^{\ell+2} - \tilde{\mathbf{e}}_h^{\ell+1})\|_2^2 - \|\nabla_h (2\tilde{\mathbf{e}}_h^{\ell+1} - \tilde{\mathbf{e}}_h^\ell)\|_2^2 \\ & \leq Ck \left( \|\nabla_h \tilde{\mathbf{e}}_h^{\ell+2}\|_2^2 + \|\nabla_h \tilde{\mathbf{e}}_h^{\ell+1}\|_2^2 + \|\nabla_h \tilde{\mathbf{e}}_h^\ell\|_2^2 + \|\tilde{\mathbf{e}}_h^{\ell+2}\|_2^2 + \|\tilde{\mathbf{e}}_h^{\ell+1}\|_2^2 + \|\tilde{\mathbf{e}}_h^\ell\|_2^2 \right) \\ & + Ck(k^4 + h^4). \end{aligned}$$

In turn, an application of discrete Gronwall inequality (in Lemma 2.2) yields the desired convergence estimate for  $\tilde{\mathbf{e}}_h$ :

$$\|\tilde{\mathbf{e}}_h^n\|_2^2 + \|\nabla_h \tilde{\mathbf{e}}_h^n\|_2^2 \leq CT e^{CT} (k^4 + h^4), \quad \text{for all } n : n \leq \left\lfloor \frac{T}{k} \right\rfloor,$$

i.e.,

$$\|\tilde{\mathbf{e}}_h^n\|_2 + \|\nabla_h \tilde{\mathbf{e}}_h^n\|_2 \leq C(k^2 + h^2).$$

An application of Lemma 2.1, as well as the time step constraint  $k \leq Ch$ , leads to

$$\begin{aligned} \|\tilde{\mathbf{e}}_h^n\|_\infty & \leq \frac{\|\tilde{\mathbf{e}}_h^n\|_2}{h^{d/2}} \leq \frac{C(k^2 + h^2)}{h^{d/2}} \leq \frac{1}{6}, \\ \|\nabla_h \tilde{\mathbf{e}}_h^n\|_\infty & \leq \frac{\|\nabla_h \tilde{\mathbf{e}}_h^n\|_2}{h^{d/2}} \leq \frac{C(k^2 + h^2)}{h^{d/2}} \leq \frac{1}{6}, \end{aligned} \tag{2.61}$$

so that the second part of the *a priori* assumption (2.40) has been recovered at time step  $k = n$ . In turn, the  $W_h^{1,\infty}$  bound (2.42) becomes available, which enables us to apply (2.20) in Lemma 2.5, and obtain the desired convergence estimate for  $\mathbf{e}_h^n$ :

$$\begin{aligned} \|\mathbf{e}_h^n\|_2 & \leq 2\|\tilde{\mathbf{e}}_h^n\|_2 + \mathcal{O}(h^2) \leq C(k^2 + h^2), \\ \|\nabla_h \mathbf{e}_h^n\|_2 & \leq C(\|\nabla_h \tilde{\mathbf{e}}_h^n\|_2 + \|\tilde{\mathbf{e}}_h^n\|_2) + \mathcal{O}(h^2) \leq C(k^2 + h^2). \end{aligned}$$

Similar to the derivation of (2.61), we also get

$$\|\mathbf{e}_h^n\|_\infty \leq \frac{1}{6}, \quad \|\nabla_h \mathbf{e}_h^n\|_\infty \leq \frac{1}{6},$$

so that the first part of the *a priori* assumption (2.40) has been recovered at time step  $k = \ell + 2$ . This completes the proof of Theorem 2.2.  $\square$

**Remark 2.3.** The regularity assumption for the exact solution, namely  $\mathbf{m}_e \in C^3([0, T]; C^1) \cap C^1([0, T]; C^3) \cap L^\infty([0, T]; C^5)$ , as stated in Theorem 2.2, is very strong. In fact, a global-in-time weak solution of the LL equation (2.1) is only of regularity class  $L^\infty([0, T]; H^1) \cap L^2([0, T]; H^3)$ . Of course, if the initial data is smooth enough, one could always derive a local-in-time exact solution with higher enough regularity estimate, so that the convergence estimate established in Theorem 2.2 could pass through. In other words, the optimal rate error estimate (2.12) stands for a local-in-time theoretical result. In

addition, since the finite difference numerical method is evaluated at the collocation grid points, instead of the ones based on a weak formulation, it usually requires higher order regularity requirement for the exact solution in the optimal rate convergence estimate than that of the finite element approach; see the related finite difference analysis for various gradient flows [8,47,49], etc.

### 3. Numerical examples

In this section, we perform 1D and 3D numerical experiments for the final time  $T = 1$  to verify the theoretical analysis in Section 2. Rate of convergence is obtained via the least-squares fitting for a sequence of error data recorded with successive stepsize refinements.

In details, we test four examples: 1D example with a forcing term and the given exact solution, 1D example without the exact solution, 3D example with a forcing term and the given exact solution, and 3D example with the full Landau-Lifshitz equation for simulating domain wall dynamics. Solutions in these four cases satisfy the homogenous Neumann boundary condition (2.2). In the presence of an forcing term, the LL equation reads as

$$m_t = -m \times \Delta m - \alpha m \times (m \times \Delta m) + f,$$

with  $f = \partial_t m_e + m_e \times \Delta m_e + \alpha m_e \times (m_e \times \Delta m_e)$  and  $m_e$  the exact solution. In more details, the forcing term  $f$  is evaluated at  $t^{n+2}$  in the numerical scheme (2.7). Only one linear system of equations needs to solve at each time step. In all examples, we find that the scheme is unconditionally stable.

**Example 3.1** (1D example with the given exact solution). The exact solution is given by  $m_e = (\cos(x^2(1-x)^2) \sin t, \sin(x^2(1-x)^2) \sin t, \cos t)^T$ , which satisfies the homogeneous Neumann boundary condition. A point-wise interpolation is applied to  $m_e(\cdot, t = 0)$  to obtain the initial data at the grid points, following formula (2.4). Results in Table 1 and Fig. 2 suggest the second-order accuracy in both time and space of the proposed numerical method in the discrete  $H^1$ -norm; Results in Table 2 indicate the unconditional stability in the 1D case.

**Example 3.2** (1D example without the exact solution). For this example, in the absence of the forcing term, we do not have the exact solution. For comparison, we first set  $h$  and  $k$  small enough to obtain a numerical solution which will be used as the reference solution. The initial condition is chosen as  $m_0(x, 0) = (0, 0, 1)^T$  for  $x \in \Omega$ . To get the temporal accuracy, we set  $h = 1D - 4$  and  $k = 1D - 4$  to get the reference solution and then record the temporal error with varying  $k$  in Table 3 and Fig. 3a. To get the spatial accuracy, we set  $h = 1/3^8$  and  $k = 1D - 4$  to get the reference solution and record the error in Table 4 and Fig. 3b. Again, the second-order accuracy in both time and space in the discrete  $H^1$ -norm have been confirmed.

**Example 3.3** (3D example with the given exact solution). The given exact solution is given by

$$m_e = (\cos(XYZ) \sin t, \sin(XYZ) \sin t, \cos t)^T,$$

where  $X = x^2(1-x)^2$ ,  $Y = y^2(1-y)^2$ ,  $Z = z^2(1-z)^2$ . Again, a point-wise interpolation is applied to  $m_e(\cdot, t = 0)$  to obtain the initial data at the grid points, following formula (2.4).

Table 5, Table 6 and Fig. 4 shows the second-order convergence in both time and space in the 3D case. Results in Table 7 indicate the unconditional stability of the proposed numerical method in the 3D case. We visualize the magnetization in Fig. 5 by taking a slice along the  $z = 1/2$  plane up to the final time  $T = 1$ . The arrow denotes the vector from magnetization component  $u$  to  $v$  and the colormap represents the third magnetization component  $w$ . Fig. 5a and Fig. 5b plot the exact magnetization with the exact value of the third component being 0.5403 and the numerical magnetization with  $k = 1/256$  and  $h_x = h_y = h_z = 1/32$ , respectively.

**Example 3.4** (3D example for full Landau-Lifshitz equation). The full Landau-Lifshitz equation in a nondimensionalized form is given by

$$\partial_t m = -m \times h_{\text{eff}} - \alpha m \times (m \times h_{\text{eff}}),$$

where the effective field  $h_{\text{eff}}$  includes not only the exchange field  $\Delta m$ , but also the anisotropy field, the external field  $h_e$  and the demagnetization (stray) field  $h_s$ . The uniaxial material with the  $x$  axis as the easy direction is considered, thus

$$h_{\text{eff}} = \epsilon \Delta m - Q(m_2 e_2 + m_3 e_3) + h_s + h_e,$$

where  $\epsilon$  and  $Q$  are both dimensionless constants,  $e_2 = (0, 1, 0)$  and  $e_3 = (0, 0, 1)$  are unit vectors,  $h_s$  takes the nondimensionalized form

$$h_s = \frac{1}{4\pi} \nabla \int_{\Omega} \nabla \left( \frac{1}{|x - y|} \right) \cdot m(y) dy,$$

**Table 1**  
Accuracy of the proposed numerical method in the 1D case on the uniform mesh when  $h = k$  and  $\alpha = 0.01$ .

$k$	$\ \mathbf{m}_h - \mathbf{m}_e\ _\infty$	$\ \mathbf{m}_h - \mathbf{m}_e\ _2$	$\ \mathbf{m}_h - \mathbf{m}_e\ _{H^1}$
5.0D-3	3.867D-5	4.115D-5	1.729D-4
2.5D-3	7.976D-6	1.053D-5	4.629D-5
1.25D-3	2.135D-6	2.648D-6	1.177D-5
6.25D-4	5.765D-7	6.627D-7	2.949D-6
3.125D-4	1.447D-7	1.657D-7	7.370D-7
order	1.991	1.990	1.972

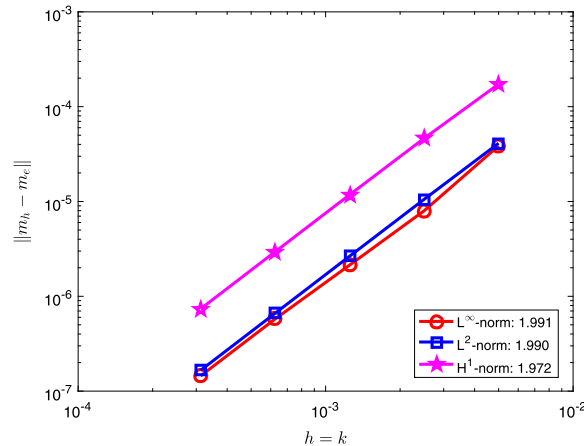


**Fig. 2.** Accuracy of the proposed numerical method on the uniform mesh when  $h = k$  and  $\alpha = 0.01$  in the 1D case.

**Table 2**  
Unconditional stability of the proposed numerical method in the 1D case when  $\alpha = 0.01$ .

$\ \mathbf{m}_h - \mathbf{m}_e\ _\infty$ \ $h$	1.0D-1	5.0D-2	2.5D-2	1.25D-2
$k$				
2.0D-1	2.318D-2	2.106D-2	2.056D-2	2.046D-2
1.0D-1	1.015D-2	7.571D-3	6.928D-3	6.768D-3
5.0D-2	5.503D-3	2.807D-3	2.134D-3	1.966D-3
2.5D-2	4.166D-3	1.436D-3	7.521D-4	5.811D-4
1.25D-2	3.783D-3	1.062D-3	3.913D-4	2.234D-4
6.25D-3	3.709D-3	9.714D-4	2.831D-4	1.108D-4

**Table 3**  
Temporal accuracy of the proposed numerical method in the 1D case on the uniform mesh when  $h = 1D - 4$  and  $\alpha = 0.01$ . The reference solution is obtained with  $h = 1D - 4$  and  $k = 1D - 4$ .

$k$	$\ \mathbf{m}_h - \mathbf{m}_e\ _\infty$	$\ \mathbf{m}_h - \mathbf{m}_e\ _2$	$\ \mathbf{m}_h - \mathbf{m}_e\ _{H^1}$
5.0D-3	2.949D-5	3.250D-5	1.633D-4
2.5D-3	8.116D-6	8.429D-6	4.393D-5
1.25D-3	2.125D-6	2.114D-6	1.118D-5
6.25D-4	4.851D-7	5.190D-7	2.791D-6
3.125D-4	1.129D-7	1.196D-7	6.875D-7
order	2.012	2.019	1.976

which is calculated by the Fast Fourier Transform (FFT) with  $\Omega$  being the rectangular domain.

Consider a ferromagnetic nanostrip of size  $0.8 \times 0.1 \times 0.004 \mu\text{m}^3$  with  $128 \times 32 \times 2$  grid points. In our simulations, the material parameters used for Permalloy, which is an alloy of Nickel (80%) and Iron (20%), are the exchange constant  $1.3 \times 10^{-11} \text{J/m}$ , the anisotropy constant  $1.0 \times 10^2 \text{J/m}^3$ , the saturation magnetization constant  $8.0 \times 10^5 \text{A/m}$ , the damping coefficient  $\alpha = 0.1$  and the temporal step-size  $k = 1 \text{ps}$ . A steady state is reached if the relative change in the total energy is less than  $10^{-7}$ . A transverse domain wall is formed with the in plane head-to-head Néel wall as the initial state (Fig. 6a), specified by

$$\mathbf{m}_h^0 = (\tanh(s), \text{sech}(s), 0)^T,$$

**Table 4**  
Spatial accuracy of the proposed numerical method in the 1D case on the uniform mesh when  $k = 1D - 4$  and  $\alpha = 0.01$ . The reference solution is obtained with  $h = 1/3^8$  and  $k = 1D - 4$ .

$h$	$\ \mathbf{m}_h - \mathbf{m}_e\ _\infty$	$\ \mathbf{m}_h - \mathbf{m}_e\ _2$	$\ \mathbf{m}_h - \mathbf{m}_e\ _{H^1}$
$1/3^2$	0.00546	0.00577	0.01336
$1/3^3$	6.101D-4	6.430D-4	0.00160
$1/3^4$	6.782D-5	7.146D-5	1.820D-4
$1/3^5$	7.527D-6	7.930D-6	2.036D-5
$1/3^6$	8.271D-7	8.714D-7	2.243D-6
order	2.001	2.002	1.980

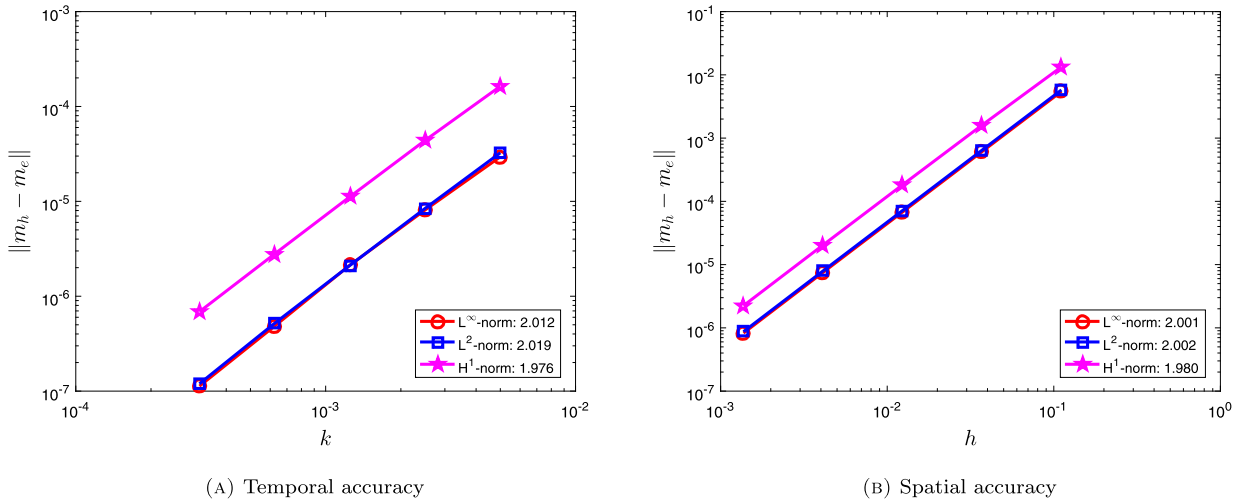


**Fig. 3.** Accuracy of the proposed numerical method when  $\alpha = 0.01$  in the 1D case. (a) Temporal accuracy of our method on the uniform mesh when  $h = 1D - 4$  and  $\alpha = 0.01$ . The reference solution is obtained with  $h = 1D - 4$  and  $k = 1D - 4$ ; (b) Spatial accuracy of the proposed numerical method on the uniform mesh when  $k = 1D - 4$  and  $\alpha = 0.01$ . The reference solution is obtained with  $h = 1/3^8$  and  $k = 1D - 4$ .

**Table 5**  
Temporal accuracy in the 3D case when  $h_x = h_y = h_z = 1/32$  and  $\alpha = 0.01$ .

$k$	$\ \mathbf{m}_h - \mathbf{m}_e\ _\infty$	$\ \mathbf{m}_h - \mathbf{m}_e\ _2$	$\ \mathbf{m}_h - \mathbf{m}_e\ _{H^1}$
1/16	1.685D-3	1.098D-3	1.211D-3
1/32	4.411D-4	2.964D-4	3.082D-4
1/64	1.128D-4	7.730D-5	7.772D-5
1/128	2.966D-5	2.024D-5	2.051D-5
1/256	8.311D-6	5.693D-6	5.812D-6
order	1.922	1.906	1.932

**Table 6**  
Spatial accuracy in the 3D case when  $k = 1/2048$  and  $\alpha = 0.01$ .

$h$	$\ \mathbf{m}_h - \mathbf{m}_e\ _\infty$	$\ \mathbf{m}_h - \mathbf{m}_e\ _2$	$\ \mathbf{m}_h - \mathbf{m}_e\ _{H^1}$
1/2	3.283D-4	2.252D-4	2.252D-4
1/4	7.442D-5	5.122D-5	6.660D-5
1/8	1.858D-5	1.278D-5	1.628D-5
1/16	4.740D-6	3.252D-6	4.048D-6
order	2.034	2.034	1.943

where  $\tanh(s) = [\exp(s) - \exp(-s)] / [\exp(s) + \exp(-s)]$  and  $\operatorname{sech}(s) = 2 / [\exp(s) + \exp(-s)]$  with  $s = [L_x/2 - x] / 2h_x$ ,  $L_x$  being the maximum length in  $x$ -direction. The transverse wall starts to move along the  $x$  direction in the presence of a small external field along the  $x$  direction with strength  $H_e = 50$  Oe. The wall profile is sustained during the motion. Snapshots at time  $t = 0.5$  ns, 1.0 ns are shown in Figs. 6b and 6c. Details of the implementation can be found in [50].

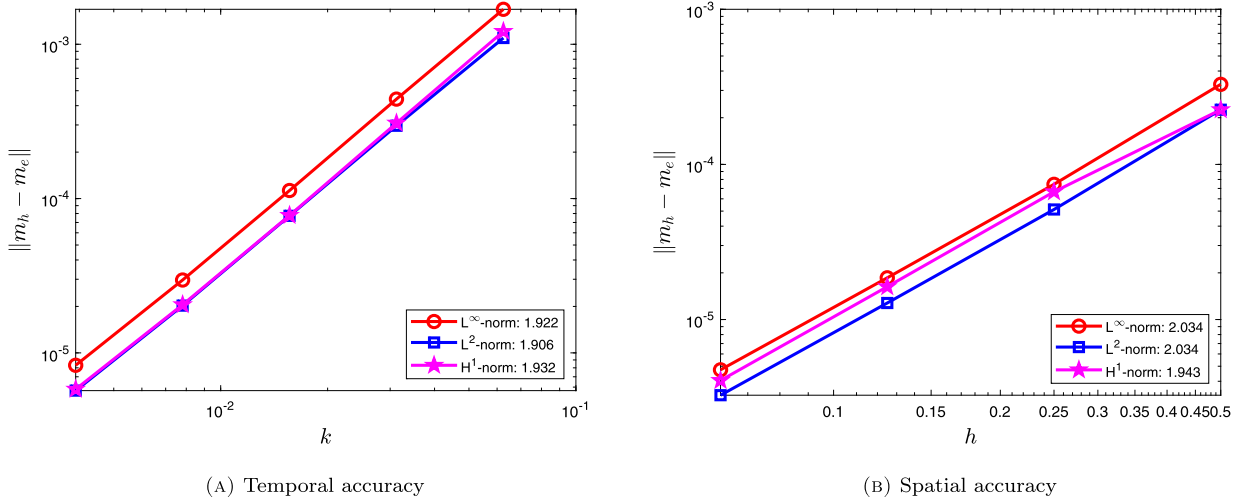


**Fig. 4.** Accuracy of the proposed numerical method when  $\alpha = 0.01$  in the 3D case. (a) Temporal accuracy of our method on the uniform mesh when  $h_x = h_y = h_z = 1/32$  and  $\alpha = 0.01$ ; (b) Spatial accuracy of the proposed numerical method on the uniform mesh when  $k = 1/2048$  and  $\alpha = 0.01$ .

**Table 7**  
Unconditional stability of the proposed numerical method in the 3D case when  $\alpha = 0.01$ .

$\frac{\ m_h - m_e\ _\infty}{h}$	$h$	1/4	1/8	1/16	1/32
1/4	$k$	1.370D-2	1.365D-2	1.370D-2	1.421D-2
1/8		5.470D-3	5.415D-3	5.407D-3	5.686D-3
1/16		1.675D-3	1.619D-3	1.605D-3	1.685D-3
1/32		5.052D-4	4.495D-4	4.355D-4	4.411D-4
1/64		1.860D-4	1.303D-4	1.163D-4	1.128D-4
1/128		1.029D-4	4.680D-5	3.311D-5	2.966D-5

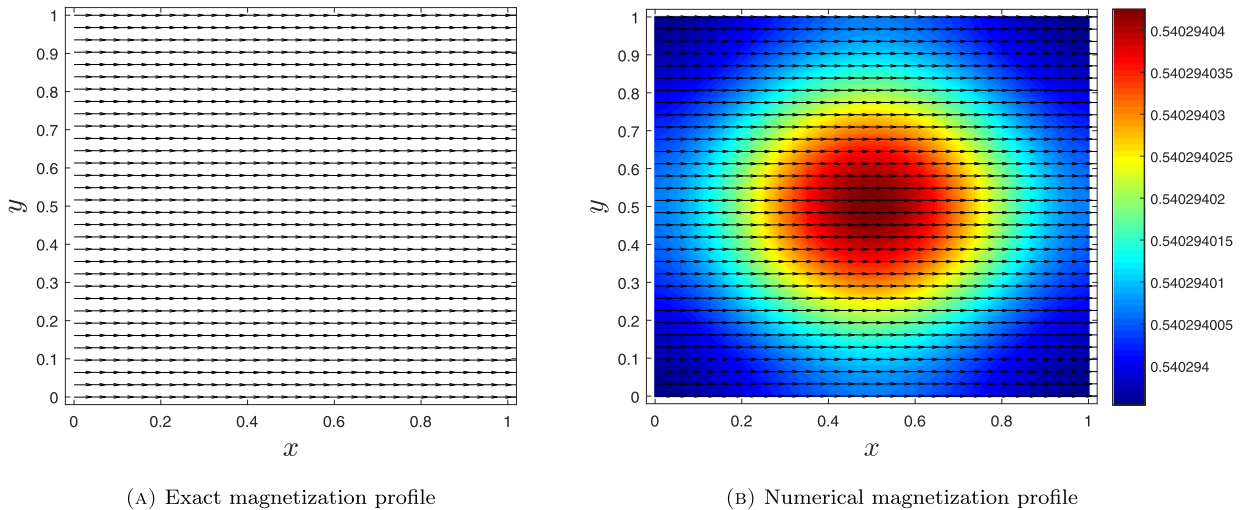


**Fig. 5.** Profiles of the exact and the numerical magnetization upon  $T = 1$  in the  $xy$ -plane with  $z = 1/2$ ,  $k = 1/256$ ,  $h_x = h_y = h_z = 1/32$ , and  $\alpha = 0.01$ . (For interpretation of the colors in the figure(s), the reader is referred to the web version of this article.)

#### 4. Conclusions

In this paper, we have proposed and analyzed a second-order time stepping scheme to solve the LL equation. The second-order BDF is applied for temporal discretization and a linearized multistep approximation is used for the nonlinear coefficients on the right hand side of the equation. The resulting scheme avoids a well-known difficulty associated with the nonlinearity of the system, and its unique solvability is established via the monotonicity analysis of the system. In addition, an optimal rate convergence analysis is provided, by making use of a linearized stability analysis for the numerical error functions, in which the  $W_h^{1,\infty}$  error estimate at the projection step has played an important role. Numerical experiments in

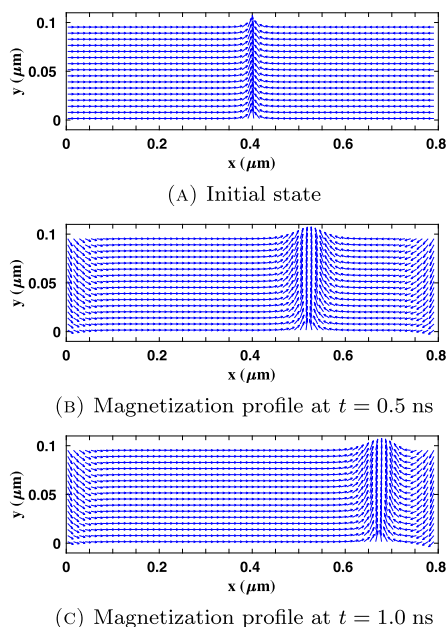


**Fig. 6.** Snapshots of the domain wall motion for the bottom surface in  $xy$ -plane of the strip with the magnetic field  $H_e = 50$  Oe along the  $x$  direction and the damping constant  $\alpha = 0.1$  at several times  $t = 0.0$  ns,  $0.5$  ns,  $1.0$  ns in (a),(b) and (c).

both 1D and 3D cases are presented to verify the unconditional stability and the second-order accuracy in both space and time, and applied to the domain wall dynamics driven by an external field. The technique presented here may be applicable to the model for current-driven domain wall dynamics [13], which shall be explored as a future project.

### Acknowledgements

We thank Zhennan Zhou from Peking University for helpful discussions. This work is supported in part by the grants NSFC 11971021 (J. Chen), NSF DMS-2012669 (C. Wang), and the Innovation Program for postgraduates in Jiangsu province via grant SJKY19\_2258 (C. Xie).

### References

- [1] C. Abert, G. Hrkac, M. Page, D. Praetorius, M. Ruggeri, D. Suess, Spin-polarized transport in ferromagnetic multilayers: an unconditionally convergent FEM integrator, *Comput. Math. Appl.* 68 (6) (2014) 639–654.
- [2] F. Alouges, A new finite element scheme for Landau-Lifshitz equations, *Discrete Contin. Dyn. Syst., Ser. S* 1 (2) (2008) 187–196.
- [3] F. Alouges, P. Jaisson, Convergence of a finite element discretization for the Landau-Lifshitz equations in micromagnetism, *Math. Models Methods Appl. Sci.* 16 (02) (2006) 299–316.
- [4] F. Alouges, E. Kritsikis, J. Steiner, J. Toussaint, A convergent and precise finite element scheme for Landau-Lifshitz-Gilbert equation, *Numer. Math.* 128 (3) (2014) 407–430.
- [5] F. Alouges, E. Kritsikis, J. Toussaint, A convergent finite element approximation for Landau-Lifshitz-Gilbert equation, *Physica B* 407 (9) (2012) 1345–1349.
- [6] F. Alouges, A. Soyeur, On global weak solutions for Landau-Lifshitz equations: existence and nonuniqueness, *Nonlinear Anal.* 18 (11) (1992) 1071–1084.
- [7] S. Bartels, A. Prohl, Convergence of an implicit finite element method for the Landau-Lifshitz-Gilbert equation, *SIAM J. Numer. Anal.* 44 (4) (2006) 1405–1419.
- [8] A. Baskaran, J. Lowengrub, C. Wang, S. Wise, Convergence analysis of a second order convex splitting scheme for the modified phase field crystal equation, *SIAM J. Numer. Anal.* 51 (2013) 2851–2873.
- [9] G. Bertotti, C. Serpico, I.D. Mayergoyz, Nonlinear magnetization dynamics under circularly polarized field, *Phys. Rev. Lett.* 86 (4) (2001) 724.
- [10] F. Browder, Nonlinear elliptic boundary value problems, *Bull. Am. Math. Soc.* 69 (1963) 862–874.
- [11] G. Carbou, P. Fabrie, Regular solutions for Landau-Lifshitz equation in a bounded domain, *Differ. Integral Equ.* 14 (2) (2001) 213–229.
- [12] G. Carbou, P. Fabrie, Regular solutions for Landau-Lifshitz equation in  $\mathbb{R}^3$ , *Commun. Appl. Anal.* 5 (1) (2001) 17–30.
- [13] J. Chen, C.J. García-Cervera, X. Yang, A mean-field model of spin dynamics in multilayered ferromagnetic media, *Multiscale Model. Simul.* 13 (2015) 551–570.
- [14] P.G. Ciarlet, *The Finite Element Method for Elliptic Problems*, Elsevier Science, 1978.
- [15] I. Cimrák, Error estimates for a semi-implicit numerical scheme solving the Landau-Lifshitz equation with an exchange field, *IMA J. Numer. Anal.* 25 (3) (2005) 611–634.
- [16] I. Cimrák, A survey on the numerics and computations for the Landau-Lifshitz equation of micromagnetism, *Arch. Comput. Methods Eng.* 15 (3) (2008) 277–309.
- [17] I. Cimrák, Convergence result for the constraint preserving mid-point scheme for micromagnetism, *J. Comput. Appl. Math.* 228 (1) (2009) 238–246.
- [18] I. Cimrák, M. Slodička, An iterative approximation scheme for the Landau-Lifshitz-Gilbert equation, *J. Comput. Appl. Math.* 169 (1) (2004) 17–32.

- [19] M. d'Aquino, C. Serpico, G. Miano, Geometrical integration of Landau–Lifshitz–Gilbert equation based on the mid-point rule, *J. Comput. Phys.* 209 (2) (2005) 730–753.
- [20] W. E, X. Wang, Numerical methods for the Landau–Lifshitz equation, *SIAM J. Numer. Anal.* 38 (2001) 1647–1665.
- [21] M. Feischl, T. Thanh, The eddy current-LLG equations: FEM-BEM coupling and a priori error estimates, *SIAM J. Numer. Anal.* 55 (4) (2017) 1786–1819.
- [22] G. Di Fratta, C.M. Pfeiler, D. Praetorius, M. Ruggeri, B. Stifftner, Linear second-order IMEX-type integrator for the (eddy current) Landau–Lifshitz–Gilbert equation, *IMA J. Numer. Anal.* 40 (4) (2020) 2802–2838.
- [23] A. Fuwa, T. Ishiwata, M. Tsutsumi, Finite difference scheme for the Landau–Lifshitz equation, *Jpn. J. Ind. Appl. Math.* 29 (1) (2012) 83–110.
- [24] H. Gao, Optimal error estimates of a linearized backward Euler FEM for the Landau–Lifshitz equation, *SIAM J. Numer. Anal.* 52 (5) (2014) 2574–2593.
- [25] V. Girault, P.A. Raviart, *Finite Element Methods for Navier–Stokes Equations, Theorems and Algorithms*, Springer-Verlag, 1986.
- [26] B. Guo, S. Ding, *Landau–Lifshitz Equations*, vol. 1, World Scientific, 2008.
- [27] B. Guo, M. Hong, The Landau–Lifshitz equation of the ferromagnetic spin chain and harmonic maps, *Calc. Var. Partial Differ. Equ.* 1 (3) (1993) 311–334.
- [28] D. Jeong, J. Kim, A Crank–Nicolson scheme for the Landau–Lifshitz equation without damping, *J. Comput. Appl. Math.* 234 (2) (2010) 613–623.
- [29] D. Jeong, J. Kim, An accurate and robust numerical method for micromagnetics simulations, *Curr. Appl. Phys.* 14 (3) (2014) 476–483.
- [30] J.S. Jiang, H.G. Kaper, G.K. Leaf, Hysteresis in layered spring magnets, *Discrete Contin. Dyn. Syst., Ser. B* 1 (2001) 219–323.
- [31] E. Kim, K. Lipnikov, The mimetic finite difference method for the Landau–Lifshitz equation, *J. Comput. Phys.* 328 (2017) 109–130.
- [32] P. Krishnaprasad, X. Tan, Cayley transforms in micromagnetics, *Physica B* 306 (1–4) (2001) 195–199.
- [33] E. Kritsikis, A. Vaysset, L.D. Buda-Prejbeanu, F. Alouges, J.C. Toussaint, Beyond first-order finite element schemes in micromagnetics, *J. Comput. Phys.* 256 (2014) 357–366.
- [34] M. Kružík, A. Prohl, Recent developments in the modeling, analysis, and numerics of ferromagnetism, *SIAM Rev.* 48 (3) (2006) 439–483.
- [35] L.D. Landau, E.M. Lifshitz, On the theory of the dispersion of magnetic permeability in ferromagnetic bodies, *Phys. Z. Sowjetunion* 63 (9) (1935) 153–169.
- [36] D. Lewis, N. Nigam, Geometric integration on spheres and some interesting applications, *J. Comput. Appl. Math.* 151 (1) (2003) 141–170.
- [37] S. Maekawa, *Concepts in Spin Electronics*, Oxford University Press, 2006.
- [38] C. Melcher, Global solvability of the Cauchy problem for the Landau–Lifshitz–Gilbert equation in higher dimensions, *Indiana Univ. Math. J.* 61 (2012) 1175–1200.
- [39] G. Minty, On a monotonicity method for the solution of non-linear equations in Banach spaces, *Proc. Natl. Acad. Sci. USA* 50 (1963) 1038–1041.
- [40] A. Prohl, *Computational Micromagnetism*, B.G. Teubner, Stuttgart, 2001.
- [41] A. Romeo, G. Finocchio, M. Carpentieri, L. Torres, G. Consolo, B. Azzerboni, A numerical solution of the magnetization reversal modeling in a permalloy thin film using fifth order Runge–Kutta method with adaptive step size control, *Physica B* 403 (2–3) (2008) 464–468.
- [42] R. Samelson, R. Temam, C. Wang, S. Wang, Surface pressure Poisson equation formulation of the primitive equations: numerical schemes, *SIAM J. Numer. Anal.* 41 (2003) 1163–1194.
- [43] T. Shinjo, *Nanomagnetism and Spintronics*, Elsevier, 2009.
- [44] A. Visintin, On Landau–Lifshitz equations for ferromagnetism, *Jpn. J. Ind. Appl. Math.* 2 (1) (1985) 69–84.
- [45] C. Wang, J.-G. Liu, Convergence of gauge method for incompressible flow, *Math. Comput.* 69 (2000) 1385–1407.
- [46] C. Wang, J.-G. Liu, H. Johnston, Analysis of a fourth order finite difference method for incompressible Boussinesq equation, *Numer. Math.* 97 (2004) 555–594.
- [47] C. Wang, S.M. Wise, An energy stable and convergent finite-difference scheme for the modified phase field crystal equation, *SIAM J. Numer. Anal.* 49 (2011) 945–969.
- [48] X. Wang, C.J. García-Cervera, W. E, A Gauss–Seidel projection method for micromagnetics simulations, *J. Comput. Phys.* 171 (1) (2001) 357–372.
- [49] S.M. Wise, C. Wang, J. Lowengrub, An energy stable and convergent finite-difference scheme for the phase field crystal equation, *SIAM J. Numer. Anal.* 47 (2009) 2269–2288.
- [50] C. Xie, C.J. García-Cervera, C. Wang, Z. Zhou, J. Chen, Second-order semi-implicit methods for micromagnetics simulations, *J. Comput. Phys.* 404 (2020) 109104.
- [51] H. Yamada, N. Hayashi, Implicit solution of the Landau–Lifshitz–Gilbert equation by the Crank–Nicolson method, *J. Magn. Soc. Jpn.* 28 (28) (2004) 924–931.
- [52] Y. Zhou, B. Guo, S. Tan, Existence and uniqueness of smooth solution for system of ferromagnetic chain, *Sci. China Ser. A, Math.* 34 (3) (1991) 257–266.